

## Giant mounded drifts in the Argentine Continental Margin: Origins, and global implications for the history of thermohaline circulation

F.J. Hernández-Molina<sup>a,\*</sup>, M. Paterlini<sup>b</sup>, L. Somoza<sup>c</sup>, R. Violante<sup>b</sup>, M.A. Arecco<sup>d</sup>, M. de Isasi<sup>d</sup>, M. Rebesco<sup>e</sup>, G. Uenzelmann-Neben<sup>f</sup>, S. Neben<sup>g</sup>, P. Marshall<sup>d</sup>

<sup>a</sup> Facultad de Ciencias del Mar, Universidad de Vigo, 36200 Vigo, Spain

<sup>b</sup> Servicio de Hidrografía Naval (SHN), Montes de Oca 2124, Buenos Aires C1270ABV, Argentina

<sup>c</sup> Instituto Geológico y Minero de España (IGME), c/Ríos Rosas, 23, 28003 Madrid, Spain

<sup>d</sup> Argentine National Commission of the Outer Limit of the Continental Shelf (COPLA), Montes de Oca 2124, Buenos Aires, C1270ABV, Argentina

<sup>e</sup> Istituto Nazionale di Oceanografia e di Geofisica Sperimentale (OGS), Borgo Grotta Gigante 42/C, 34010 Sgonico, Italy

<sup>f</sup> Alfred Wegener Institute (AWI), Foundation for Polar and Marine Research Geophysics, P.O. Box 12 01 61, Am Alten Hafen 26, 27515 Bremerhaven, Germany

<sup>g</sup> Bundesanstalt für Geowissenschaften und Rohstoffe (BGR), Stilleweg 2, 30665 Hannover, Germany

### ARTICLE INFO

#### Article history:

Received 13 August 2009

Received in revised form

30 December 2009

Accepted 19 April 2010

Available online 24 April 2010

#### Keywords:

Contourite drift

Slope

Seamounts

Palaeoceanography

Seismic stratigraphy

Hydrocarbon potential

Argentine Margin

### ABSTRACT

Partially buried giant drifts are located in the southern-most sector of the Argentine continental margin, generating a bathymetric jump at the base of the slope. They are characterised as giant, asymmetrical elongated, mounded contourite drifts, and are described in detail here for the first time. This description is mainly based on the bathymetric and multichannel seismic reflection profiles data. Their origin and evolution in the Argentine Basin are decoded and their implications in an area crucial for geologic and palaeoceanographic reconstruction between the Atlantic and Antarctica are discussed. The buried giant drifts are divided into two zones by a large seamount. The major giant-drift (50 km wide, 300 km long, and having a sedimentary thickness of nearly 1 km) is located to the south of this seamount and oriented to the north, where its summit outcrops at present seafloor. Here, its asymmetric external shape is characterised by a steep, western side and a gently dipping, smooth eastern side, with internal reflections prograding eastward. Based on its position, morphology and internal characteristics, it has been deduced that this giant-drift was generated in the Argentine Basin by the southward branch of a confined large loop of the Antarctic Bottom Deep Water, from the Eocene-Oligocene boundary (coevally with the Drake Passage opening) until the middle Miocene. However, after a major palaeoceanographic change in the mid-to-late Miocene a new oceanographic scenario was established that fossilised these giant drifts. These changes produced a new depositional style in the margin, resulting in initiation of the present contourite depositional system and morphologic features over the slope. Extension of North Atlantic Deep Water circulation into the Southern Hemisphere and deepening of Antarctic Bottom Water circulation in the Argentine Basin are herein postulated as the factors that controlled said changes. These giant drifts show strong seismic evidence of hydrates and free gas that are ripe for energy resources exploration, thus demonstrating the economic potential of contourite deposits in deep marine environments.

© 2010 Elsevier Ltd. All rights reserved.

### 1. Introduction

Contour-following currents generated by the thermohaline circulation (THC) are particularly marked on continental margins and abyssal plains, and are sometimes strong enough to profoundly affect sedimentation, from winnowing of fine deposits to development of large-scale depositional or erosive features (Kennett,

1982; Stow, 1994; Stow et al., 2002a; Rebesco and Camerlenghi, 2008; Stow et al., 2009). The deposits generated by such along-slope currents are known as *contourites* or *contourite drifts* and have recently been classified by several authors (McCave and Tucholke, 1986; Faugères and Stow, 1993; Faugères et al., 1993, 1999; Rebesco and Stow, 2001; Stow et al., 2002a; Rebesco, 2005; Rebesco and Camerlenghi, 2008). Various erosive features (e.g. terraces, abraded surfaces, contourite channels, contourite moats, and furrows) are locally developed in the areas in which the currents are generally stronger, and are often associated to the contourite drifts. Extensive erosion or non-deposition leads to the development of widespread hiatuses in the depositional

\* Corresponding author.

E-mail address: [fjhernan@uvigo.es](mailto:fjhernan@uvigo.es) (F.J. Hernández-Molina).

records (Van Andel et al., 1977; Laberg et al., 2005; Stoker et al., 2005; Maldonado et al., 2006). Although erosive features in contourites have been studied (see, for example: Nelson et al., 1993, 1999; Evans et al., 1998; Stow and Mayall, 2000; Masson, 2001; Hernández-Molina et al., 2006, 2008a; García et al., 2009), they have yet to be classified into a single system that incorporates standard drift categories.

Whilst interaction between down-slope and along-slope sedimentary processes is common over continental margins when along-slope processes dominate, a Contourite Depositional System (CDS) may develop as an association of various depositional features (drifts) and erosive features (Hernández-Molina et al., 2008a,b). The interaction of one or more water masses with a smooth-morphology margin may cause large drifts, but a complex physiography can create multiple vortices associated with each water mass, and both the erosive and depositional features can become difficult to decipher (Faugères et al., 1999; Stow et al., 2002a; Hernández-Molina et al., 2008a; Rebesco and Camerlenghi, 2008). Some contourite deposits represent giant, mounded elongated contourite drifts (hereafter, *giant drifts*) extending along large distances (Faugères et al., 1999; Hernández-Molina et al., 2008b; Stow et al., 2008), such as those described in the Weddell and Scotia Basins (Maldonado et al., 2003, 2006), south-westernmost Indian Ocean (Niemi et al., 2000; Uenzelmann-Neben, 2001, 2002) and Greenland margin (Hunter et al., 2007). These giant drifts are generated during a long period of relatively stable hydrological conditions that lead to long-term bottom water flows. Onset of many of these drifts is related to a gateway opening or deepening, owing to long-term plate-tectonic evolution, and/or large-scale palaeoceanographic changes associated with climatic changes. In fact, the onset of many of those located in ocean basins began in the Eocene/Oligocene boundary and became re-activated by the Middle Miocene, with the establishment of the present global THC (Kennett, 1982; Niemi et al., 2000; Flood and Giosan, 2002; Pfuhl and McCave, 2005; Knutz, 2008). Therefore, an understanding of giant drifts is essential to understanding major tectonic or palaeoceanographic changes, and consequently, to understand how the THC and climate were in the past. Moreover, they have great potential for mineral and energy resource exploration, since they are often amenable to generation of poly-metallic nodules and to accumulation of hydrates and free gas (Kennett, 1982; Viana et al., 2007; Viana, 2008).

This paper describes in detail, for the first time ever, giant drifts located on the extensional Argentine Continental Margin (Fig. 1), in the southern portion of the South Atlantic Ocean, in an area crucial for geologic and palaeoceanographic reconstruction between the Atlantic and Antarctica. Its genesis and evolution in the Argentine Basin are explained, and its global implications are discussed.

## 2. The oceanographic scenario

Interaction of highly active oceanographic processes with the seafloor is an essential characteristic of the Argentine margin, which is one of the most dynamic of the world's oceans (e.g. Chelton et al., 1990) (Fig. 1). This margin encompasses the Brazil/Malvinas Confluence (BMC), as well as the interaction of Antarctic water masses (Antarctic Intermediate Water [AAIW], Circumpolar Deep Water [CDW] and Antarctic Bottom Water [AABW]), with the Brazil Current, re-circulated AAIW and North Atlantic Deep Water (NADW) (Georgi, 1981b; Saunders and King, 1995; Piola and Matano, 2001; Carter et al., 2009) at different depths (Fig. 1). The surface circulation around the Argentine margin results from interaction of the Malvinas Current toward the north-northeast with the Brazil Current toward the south-southwest, both of which determine the BMC. The BMC strongly conditions the sedimentary

processes and the margin's morphology (Lonardi and Ewing, 1971; Piola and Rivas, 1997). The intermediate circulation south of this confluence is conditioned by the circulation toward the north of the Antarctic Intermediate Water (AAIW), and of the two CDW fractions: Upper Circumpolar Deep Water (UCDW) and Lower Circumpolar Deep Water (LCDW) (Arhan et al., 2002a,b). South of the BMC, the LCDW is divided into two high-velocity cores (1 and 2) at approximately 2500 m water depth, and the South Pacific Deep Water (SPDW) is identified below the LCDW (Arhan et al., 2002a). Northward of the confluence, apart from the aforementioned water masses, the NADW develops, circulating toward the south (Fig. 1). Interfaces among the aforementioned water masses are determined by changes in density, so that they deepen northward at basin scale, and are vertically displaced by eddies (Piola and Matano, 2001; Arhan et al., 2002a,b). These interfaces are locally shallower where the CDS is developed, due to physiographic changes in the margin (Piola, pers. comm., 2008). The CDS is located where Intermediate Water mass circulation is affected by the northward flow of AAIW, at depths shallower than 1000 m, and by the UCDW and LCDW, at depths between 1000 and 3500 m (Saunders and King, 1995; Piola and Matano, 2001). North of the BMC, NADW flows southward, close to the slope, at 1500 to 2800 m water depth (Fig. 1 and Table 1).

The deep circulation is caused by the displacement of AABW (Fig. 1), which is partially trapped in the basin, generating a large (up to 2000 m thick) cyclonic gyre, the influence of which is felt at depths greater than 3500–4000 m (Piola and Matano, 2001; Arhan et al., 2002a,b; Hernández-Molina et al., 2008b; Carter et al., 2009). This oceanographic regime is clearly significant in controlling sedimentary processes across the entire ocean basin (Le Pichon et al., 1971; Reid, 1989; Klaus and Ledbetter, 1988), and particularly on the Argentine margin (Flood and Shor, 1988; Arhan et al., 2002a,b; Hernández-Molina et al., 2009). AABW in this basin is composed of Weddell Sea Deep Water (WSDW), which enters the basin from the south through the Falkland/Malvinas gaps, and around the Falkland/Malvinas Plateau in the east, before turning westwards and passing the Malvinas/Falkland Escarpment, until finally heading northward at the Argentine continental slope (Fig. 1). AABW flows continuously north as an intensified western boundary current penetrating into the Brazil abyssal plain through the Vema and Hunter Channels (Le Pichon et al., 1971; Georgi, 1981a; Speer et al., 1992; Faugères et al., 1993; Onken, 1995; Carter et al., 2009).

## 3. Physiographic, morphologic and regional geologic settings

The extensional Argentine continental margin is one of the largest in the world (Hinz et al., 1999; Urien, 2001; Franke et al., 2007). It features a continental slope with a south-west trend until the 45° parallel, where it heads east south-east, and finally, east (Fig. 1). Between parallels 35° and 49°S, it is 1500 km long, 50–300 km wide, has an average slope gradient of ca. 2° and a total area of 700,000 km<sup>2</sup> (Lonardi and Ewing, 1971; Ewing and Lonardi, 1971; Mouzo, 1982; Parker et al., 1996, 1997). The continental rise is only well defined in the central and northern sectors of the margin, starting at depths of ca. 3200–3500 m and at a width of 250 km. It is connected with the abyssal plain (Argentine Basin) at a depth of 5000 m, and is locally crossed by various submarine canyons and valleys. The abyssal plain has a surface area of about 200,000 km<sup>2</sup>, and its deepest part along the western and south-western margins (known as the *Abyssal Gap*) reaches a maximum water depth of 6212 m (Lonardi and Ewing, 1971; Ewing and Lonardi, 1971; Parker et al., 1996, 1997). There are three huge contourite drifts (the Zapiola, Argyro and Ewing drifts, Fig. 1), which are generated by the long-term cyclonic movement of AABW and are mainly composed of silts and mud (Ewing and Lonardi, 1971; Flood and Shor, 1988;



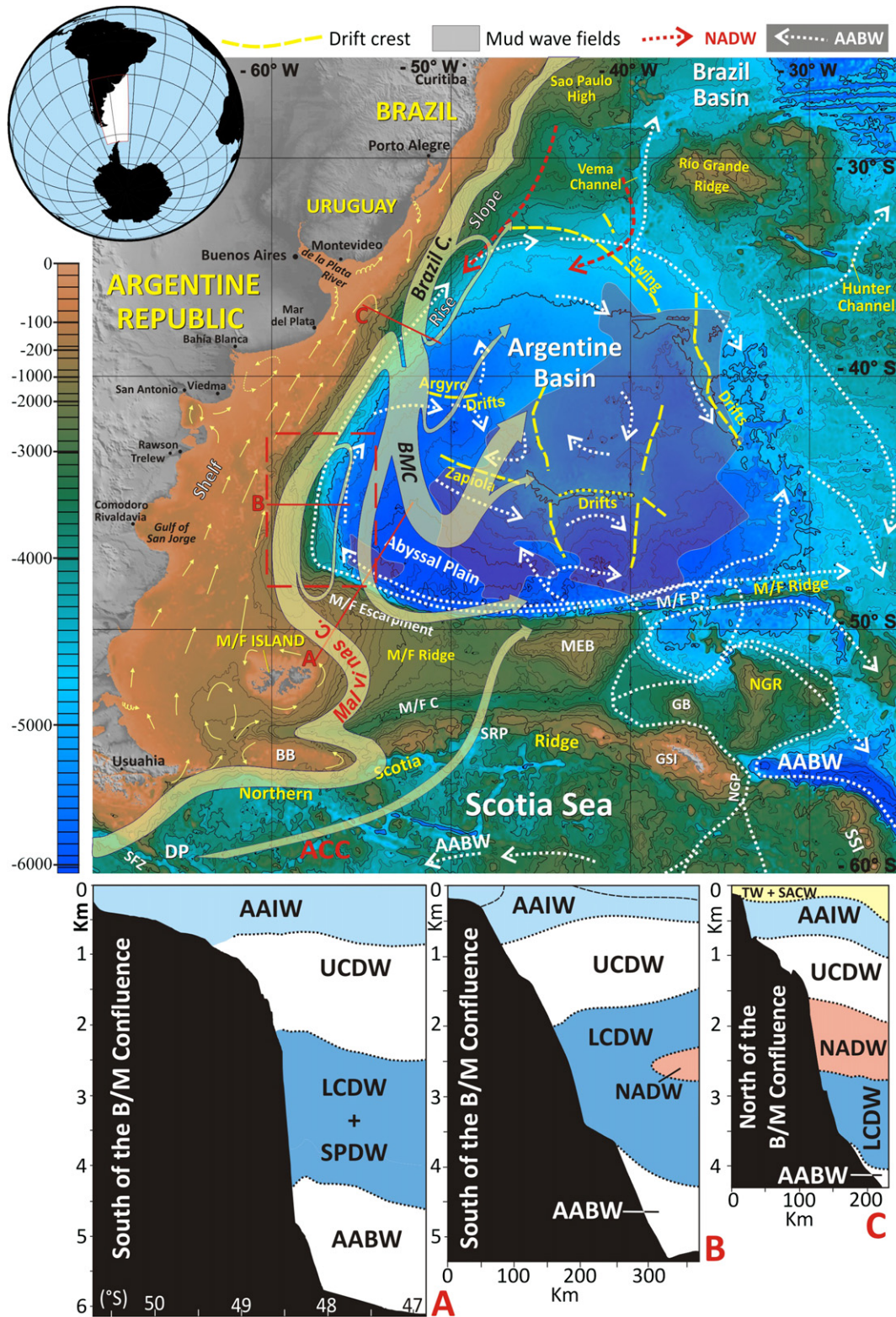


**Fig. 1.** Location of the Argentine Margin, with the regional bathymetric map and the general circulation of surface- and deep-water masses indicated (compiled from: Flood and Shor, 1988; Reid, 1989, 1996; Klaus and Ledbetter, 1988; Speer et al., 1992; Faugères et al., 1993; Piola and Rivas, 1997). Simplified hydrographic sections are shown below: (A) from Arhan et al. (2002a), and (B and C) from Piola and Matano (2001). The study area shown in Fig. 3 is represented by the dashed line of red square. Legend for the physiographic reference points, in alphabetical order: BB = Burdwood Bank; BMC = Brazil-Malvinas Confluence; DP = Drake Passage; M/Fl = Malvinas-Falkland Island; M/FE = Malvinas-Falkland Escarpment; M/FP = Malvinas-Falkland Passage; M/FR = Malvinas-Falkland Ridge; GB = Georgia Basin; GP = Georgia Passage; MEB = Maurice Ewing Bank; NGR = Northeast Georgia Passage; NGR = Northeast Georgia Ridge; SG = South Georgia; SFZ = Shackleton Fracture Zone; SRP = Shag Rocks Passage; and SSI = South Sandwich Island. Legend for the water masses: ACC = Antarctic Circumpolar Current; AABW = Antarctic Bottom Water; AAIW = Antarctic Intermediate Water; CDW = Circumpolar Deep Water; LCDW = Lower Circumpolar Deep Water; SACW = South Atlantic Central Water; SPDW = Southeast Pacific Deep Water; TW = Mass of Tropical Water; and UCDW = Upper Circumpolar Deep Water.

**Table 1**

Stratification of the different water masses in the Argentine and Brazilian Basins, indicating the depth of their interfaces. Legend for the water masses: AABW = Antarctic Bottom Water; AAIW = Antarctic Intermediate Water; BC = Brazil Current; BMC = Brazil/Malvinas Confluence Zone; CDW = Circumpolar Deep Water; LCDW = Lower Circumpolar Deep Water; SACW = South Atlantic Central Water; SPDW = Southeast Pacific Deep Water; TW = Tropical Water; UCDW = Upper Circumpolar Deep Water; and WSDW = Weddell Sea Deep Water. (Compilation based on the work of the following authors, listed in alphabetic order: Arhan et al., 2002a,b; Boebel et al., 1999; Flood and Shor, 1988; Georgi, 1981b; Klaus and Ledbetter, 1988; Lonardi and Ewing, 1971; Piola and Matano, 2001; Reid, 1989, 1996; Saunders and King, 1995; Speer et al., 1992).

ARGENTINE BASIN				BRAZILIAN BASIN		
S of the BMC		N of the BMC		BC (towards the S)		
AAIW		AAIW		IBCC (towards the N)		
1 000 m		~ 900–1 000 m		~ 1 500 m		
CDW	UCDW	UCDW	CDW	NADW In contact with the slope	UCDW	CDW No contact with the slope
	~ 1 000 m	~ 1 500 m– NADW In contact with the slope			~ 2 000– 2 200 m	
	2 000– 2 200 m	~ 2 500– 2 800 m			LCDW	
LCDW (+ SPDW)		LCDW		LCDW		
3 800 (S)–3 500 (N) m		~ 3 500 m		~ 3 500 m		
AABW (WSDW)				AABW (WSDW)		

Hernández-Molina et al., 2008b). The most prominent is the Zapiola drift, a giant, elongated-bifurcated sediment drift centred in the southern part of the basin (Fig. 1). It fills, and extends over, the abyssal plain, and is shaped like a giant, flat-lying letter “H”. It has a diameter of ca. 350 km, a maximum thickness of ca. 3000 m, curvilinear crests between 4750 and 5950 m water depth, and a relief of ca. 1200 m above the adjacent seafloor (Ewing and Lonardi, 1971; Le Pichon et al., 1971; Flood and Shor, 1988; Manley and Flood, 1993; Von Lom-Keil et al., 2002). The Argyro drift has been interpreted as a series of overlapping smaller drifts across the central part of the abyssal plain (Heezen and Tharp, 1977). The Ewing drift (Fig. 1) extends east–southeast from the South American rise into the abyssal plain toward the Zapiola drift. Its main crest line is arch-shaped; a secondary crest lies eastward of, and runs parallel to, this primary crest, following the 4000–5000 m contour. This pathway is consistent with the general pathway predicted for a return flow of abyssal water (Flood and Shor, 1988). Large parts of these drift complexes are covered by extensive sediment wave fields (Fig. 1), including some of the largest in the world, where the waves average 25–30 m (max. 150 m) in height and 5000–6000 m (max. 10000 m) in wavelength (Von Lom-Keil et al., 2002).

Along the extensional Argentine margin, the continental shelf is located on the continental crust, whereas part of the lower slope and the rise lie on the transition between the continental and the oceanic crust. This margin is considered an extensive volcanic passive margin between 35 and 49°S (since the Upper Cretaceous), characterised by a thick wedge of seaward-dipping reflectors (SDRs) located on the aforementioned transition (Light et al., 1993; Ramos, 1996; Gladczenko et al., 1997; Hinz et al., 1999; Schumann, 2002; Franke et al., 2007). Nevertheless, along the Malvinas/Falkland Escarpment, Malvinas/Falkland Fracture and Malvinas/Falkland Ridge, there is a shear fracture zone delimiting an extensive margin which bounds the Malvinas/Falkland Plateau, Maurice Ewing Bank and the Georgia Basin to the north (Fig. 1). Current tectonic characteristics have been dictated by its previous structural history, which regulated break-up processes, thermal flow and magmatic activity. The Argentine margin was recently divided into four large tectonic segments (labelled I to IV) separated by large

transfer fault zones (see Hinz et al., 1999; Franke et al., 2007). Over the course of its large-scale evolution, gravitational mass and turbiditic processes have predominated, although along-slope sedimentary processes induced by oceanic circulation have also been significant in influencing the more recent evolution of the southernmost part of the margin (Ewing and Lonardi, 1971; Lonardi and Ewing, 1971; Hernández-Molina et al., 2009).

Within the Argentine extensional margin, the Argentine Sedimentary Basin (also known as the Eastern Patagonia Basin or the Ameghino Basin) is located along the slope and rise, east of a structural high of continental crust basement. It is ca. 2300 km long (with a clear north–east trend) and 350 km wide and has a total area of ca. 800,000 km<sup>2</sup> (Ewing and Lonardi, 1971; Urien and Zambrano, 1996; Urien, 2001; Hinz et al., 1999). The sedimentary fill in this basin is over 8000 m thick, and there is a direct relationship between the large depocenters and the four large tectonic segments of the aforementioned margin (Urien and Zambrano, 1996; Hinz et al., 1999; Franke et al., 2007). The sedimentary record of the basin (Ewing and Lonardi, 1971) reveals twelve evolutionary episodes, separated by erosional surfaces with great lateral continuity. Later, four major units were divided by three regional unconformities (Urien et al., 1976), and more recently, a regional stratigraphic correlation between the Argentine and Colorado Basins was made (Hinz et al., 1999; Franke et al., 2007), enabling the proposal of a more reliable age framework, homogenisation and simplification of the previous nomenclature, and consideration of five major regional stratigraphic discontinuities for the entire margin (AR1–AR5, Table 2).

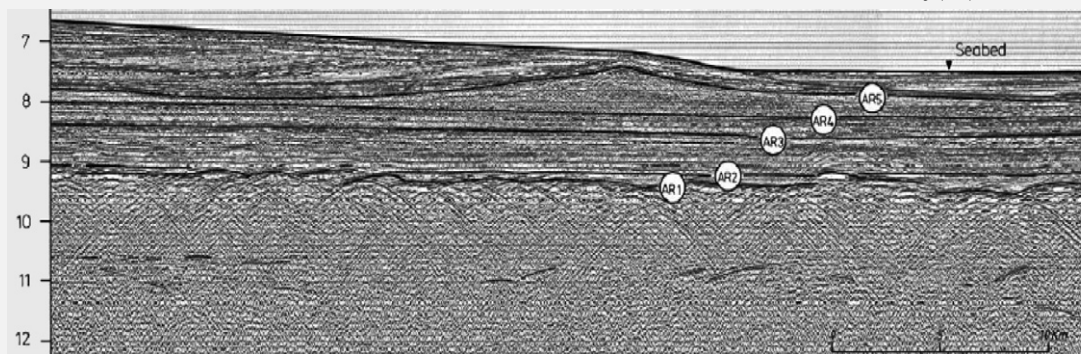
#### 4. Materials and methods

This study is primarily based on the bathymetric and multi-channel seismic reflections profiles (MCS) broad database (Fig. 2), collected and compiled during the last seven years by the *Comisión Nacional del Límite Exterior de la Plataforma Continental* (COPLA; Argentina). Bathymetric compilation of single-beam and swath bathymetric data was performed by Geosoft Oasis Montaj, including public data (ETOPO2 and GEODAS) and data from several



**Table 2**  
Regional stratigraphic discontinuities defined by Hinz et al. (1999) and Franke et al. (2007) for the Argentine continental margin. Below, details of the multichannel seismic section of the southern Segment (I), where the five regional discontinuities defined by Hinz et al. (1999) are shown. Note how Discontinuity AR4 is located at the base of the giant-drift deposits.

Urien et al. (1976)		Hinz et al. (1999)		Franke et al. (2007)	
Regional discontinuity	Attributed age	Regional discontinuity	Attributed age	Regional discontinuity	Attributed age
AR I	Middle Cenozoic (Eocene–Oligocene)	AR 5	Middle Miocene (~15 Ma)		No assigned age
AR II	Cretaceous–Cenozoic boundary	AR 4	Eocene–Oligocene boundary		No assigned age
AR III	Middle Cretaceous (Aptian)	AR 3	Upper Cretaceous (~81 Ma)		No assigned age
		AR 2	Upper Aptian	Pedro Luro equivalent (PLe)	= AR2, Cretaceous/Tertiary Limit
		AR 1	Hauterivian (~125 Ma)	Breakup Unconformity (BU)	= AR 1



cruises (e.g. Fisiso96, BGR98, BGR04, COPLA2001-2002, Litoral BONAERENSE III, TESAC, NavPD2000, ANTARKTIS-XXII/4, Marion Dufresné-2500 and BIO Hesperides-2008).

MCS profiles spaced at 55 km intervals were collected on the Argentine slope (Fig. 2) by COPLA and the *Bundesanstalt für Geowissenschaften und Rohstoffe* (BGR; Germany) during four cruises in 1998, 1999, 2001–2002, and 2004 (Hinz et al., 1988, 2000; Neben and Schreckenberger, 2005). Airguns with variable capacities (4000–5200 m<sup>3</sup>) were used as the source system. In all cruises the shooting interval was 50 m; the streamers, 6000 m long; the sampling rate, 2 ms and the recording length, from 12 to 15 s. Standard MCS profiles were processed with both pre-stack time and depth migration. The acquisition and processing parameters were chosen to ensure the quality of the seismic sections.

Bathymetric and MCS data were used for a regional morpho-sedimentary study, which enabled the production of a map of the Argentine Contourite Depositional System (Hernández-Molina et al., 2009). Recent swath bathymetry data were collected in 2008 by the Simrad EM-120 echo sounder on board the BIO-Hesperides, which followed the crest of the giant drifts outcropping at the seafloor and identified both the present seamount distribution and the base of the slope (BOS). Moreover, single-channel seismic reflection profiles, compiled by Lamont-Doherty Earth Observatory (LDEO, Columbia Univ., New York), were used for the morphologic study and for locating and characterising the giant drifts. These data were collected during cruises in the 1960s and 1970s and are available both from the Marine Geology and Geophysics Division of the Argentine Naval Hydrographical Service, and digital data set from GeoMapApp (Lamont-Doherty Earth Observatory of Columbia University, <http://www.geomapp.org>).

MCS profiles enable regional seismic stratigraphic analysis of the recent sedimentary record, together with a detailed seismic-

facies analysis of the giant drifts, which feature six seismic lines (Fig. 2): BGR 04-13, BGR 04-07; BGR 87-05; COPLA 01-23; COPLA 01-23B; COPLA 01-22 (hereafter, *Lines*, 13, 7, 5, 23, 23b, and 22, respectively, for simplicity). Correlation of the seismic units and discontinuities with seismic line BGR 87-05A from Hinz et al. (1999) was crucial to establish the age framework for the sedimentary record, including those of discontinuity AR-4 at the base of the giant drifts and the well remarkable internal discontinuity AR-5 (Hinz et al., 1999; Table 3). The deposits and associated erosional elements were interpreted as belonging to contourite drifts, according to recent classifications of drifts. The latest classification (Faugères and Stow, 2008) has been adopted, which is chiefly based on previous classifications by McCave and Tucholke (1986), Faugères et al. (1999), Rebesco and Stow (2001), Stow et al. (2002a), and Rebesco (2005).

Data on free-air gravimetric anomalies collected along the seismic profiles tracks have been considered in order to evaluate the potential local influence of the giant drifts in local gravimetric anomalies. A Bouguer anomaly was calculated by removing the water column, and assuming 2.21 g cm<sup>-3</sup> in density (Pawlowski, 2008). Regional Bouguer anomaly was calculated based on the method of Parker (1973). The horizontal gradient in the east-west direction was calculated from the Bouguer anomaly data using Geosoft Oasis Montaj software; this is a simple density variation technique for mapping short wave-length lateral anomaly changes due to local geological features with the highest values in area (Lyatsky et al., 2004). The giant drifts gravity model (corrected Bouguer anomaly) was calculated using a Fortran program according to Talwani and Ewing (1960) and the relative densities was obtained by Gardner et al. (1974). The relative density of sediments was obtained by first calculating the average velocity interval in seismic processing, and then converting this value to densities following the methodology of Gardner et al. (1974).

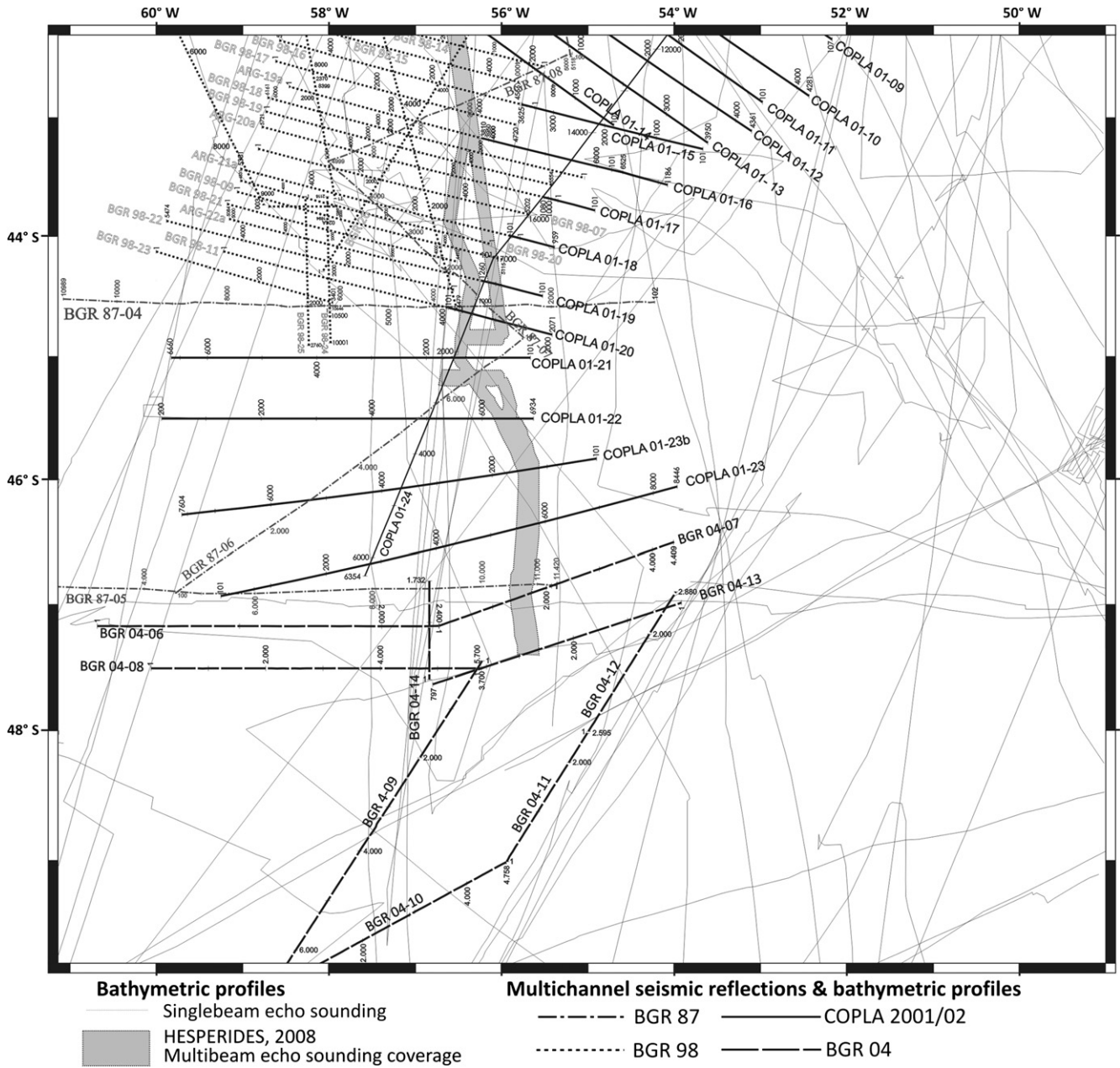


**Fig. 2.** Location of the bathymetric and multichannel seismic reflections profiles (MCS) database in the studied area. Six MCS lines are located across the giant drift: BGR 04-13, BGR 04-07; BGR 87-05; COPLA 01-23; COPLA 01-23b; COPLA 01-22. COPLA = Comisión Nacional del Límite Exterior de la Plataforma Continental; and BGR: Bundesanstalt für Geowissenschaften und Rohstoffe.

**5. Results**

*5.1. The Contourite Depositional System*

The Argentine contourite depositional system (CDS) is located in tectonic Segment I and the southernmost sector of Segment II (Segment IIa) defined by Franke et al. (2007), and therefore, between the Transfer Fracture Zones of Malvinas/Falkland (M/F) and Colorado (Segment I) and the Transfer Fracture Zones of Colorado and Bahía Blanca. The area in which the CDS is developed does not contain any continental rise; thus, the lower slope directly connects to the abyssal plain. The CDS exhibits both depositional and erosive features that delineate two major sectors (Fig. 3): the Escarpment and Terraces sector and the Submarine Canyons and

Channels sector (for further details, see Hernández-Molina et al., 2009). These sectors are not completely coincident with the boundaries of the aforementioned segments.

*5.1.1. The Escarpment and Terraces sector*

This sector is fully located within Segment I and encompasses two differentiated zones: the Escarpment zone and the Terraces zone.

The Escarpment zone is located northward of the M/F Escarpment (Fig. 3). Depositional features at the BOS are represented by mounded and plastered drifts, whereas the erosive features are characterised by small channels oblique to the escarpment (NW trending), grouped into a well-defined channel located at a depth of ca. 5 km (Fig. 3). This channel laterally connects with Contourite



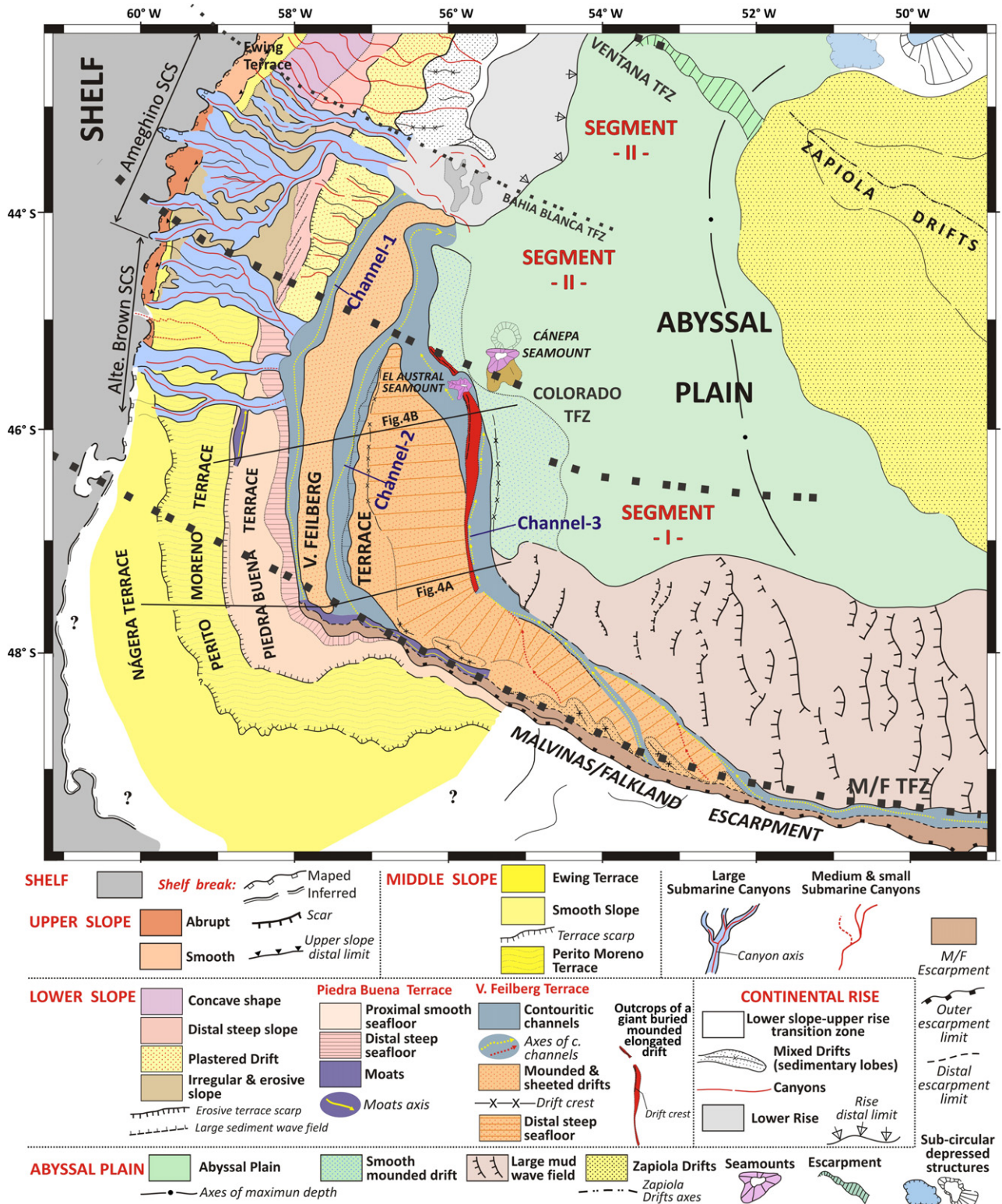


Fig. 3. Simplified morphosedimentary map of the Argentine Margin of the Argentine Contourite System; the locations of the giant drifts are shown in red (Modified from Hernández-Molina et al., 2009).

Channel 3 (hereafter, *Channel 3*). Toward the abyssal plain there is an extensive mud-wave field migrating westward, which was previously defined and mapped by Flood and Shor (1988).

The majority of this sector comprises the Terraces zone, in which erosive features dominate (Fig. 3). The predominant erosive features comprise terraces, contourite moats and channels. The terraces are

sub-horizontal morphologic elements identified at the present seafloor. They developed over time in constructional (depositional) and erosive phases (Fig. 4). A set of four terraces with major lateral continuity has been identified at different depths: *Nágera*, at 500 m; *Perito Moreno*, at 1000 m; *Piedra Buena*, at 2500 m; and *Valentin Feilberg*, at 3500–4000 m (Fig. 3 and 4). These terraces are ca. 450 km



**Table 3**

Discontinuities, seismic units and subunits within the sedimentary record of the Argentine Contourite System, summarising the major deduced paleoceanographic changes.

Major Units	Sub-Units	Attributed age	Evolutionary stages of giant drifts	Paleoceanographic implication in the Argentine Basin
Upper Unit (UU)	a	Late Pliocene + Quaternary	INACTIVE STAGE	New oceanographic scenario was established & present morphologic features began to develop
		<i>Late Pliocene?</i>		
	b	Lower Pliocene		
		<i>Late Miocene/early Lower Pliocene</i>		
	c	Late Miocene		2 <sup>nd</sup> more dramatic paleoceanographic change. CAS shoaling
<b>Discontinuity</b>		<i>Late Middle Miocene</i>		Giant-drifts became inactive
<b>Intermediate Unit (IU)</b>		Middle Miocene	VERTICAL GROWTH STAGE	1 <sup>st</sup> major paleoceanographic change. Onset of NADW & LCDW.
<b>AR-5 Discontinuity</b>		<i>Middle Miocene (~ 15 Ma)</i>		
Lower Unit (LU)	a	Oligocene - Middle Miocene	GROWTH STAGE	Aggradational phase associated with major subsidence
	b			
	c			
<b>AR-4 Discontinuity</b>		<i>Eocene – Oligocene boundary</i>		End of compressional tectonics in the Patagonia Cordillera & Re-opening and deepening of the Drake Passage
				Onset & growth stage of giant-drifts
				AABW was an intensified western boundary current
				Opening of the Drake Passage & onset of the AABW circulation

long and 50 km wide. The proximal portion has a seaward slope (0.25–0.5°), whereas across the distal portion, the sea-floor slope gradient is slightly steeper (0.5–1°). A large moat with good lateral continuity, which runs parallel to the northwest end of the M/F Escarpment, has also been identified. At ~48°S/~57°W this moat is subdivided into two contourite channels: the *Keninek* contourite channel (hereafter, *Channel-1*) and the *Kolenten* contourite channel (hereafter, *Channel-2*). Channel-1 is located at depths of 3800 m, deepens northwards and represents the landward boundary of the Valentin Feilberg terrace. It has an *ca.* 130 m incision in the south that deepens to 920 m in the north. Channel-2 is found at depths of 4000–4500 m. It is smooth at its proximal end, but quickly deepens northward, crossing the Valentin Feilberg terrace with a slightly oblique trend with respect to the slope. This channel is roughly 460 km long and 18 km wide, with a 130 m-deep incision in the south that increases to 300 m in the north. Furthermore, Channel-3 (*ca.* 300 km long and 20 km wide) is located at the distal end of the Valentin Feilberg terrace at depths of *ca.* 5000 m. It features a 210 m-deep incision to the south that decreases to 131 m to the north. Finally, a new, shorter contourite channel (*ca.* 60 km long; 8 km wide; 300–400 m-deep incision) parallel to the slope oceanward of the Piedra Buena terrace is present at 2500–3000 m depth, from 46.5°S to the Almirante (Alte.) Brown submarine canyon system (SCS). The depositional features of Segment I are located at depths greater than 4000 m at BOS. In the southernmost part of the Valentin Feilberg terrace, sheeted drifts are exhibited at depths of 3800–4500 m and change laterally northward into two mounded, elongated and separated drifts over the Valentin Feilberg terrace (Fig. 3). Toward the abyssal plain there are sheeted drifts that are marked by flat sea-bottom morphology, yet contain local progradational bodies, sediment waves and erosive scarps within the sedimentary record.

### 5.1.2. The submarine canyons and channels sector

This sector is located in the slope of the northern part of Segment I and the southernmost sector of Segment II, where erosive features are also predominant (Fig. 3). It encompasses two submarine canyon systems (SCSs) (Fig. 2). In the south, the west–northwest-trending Alte. Brown SCS crosses the slope down to a depth of 3500 m, where it joins Channel-1. At this point, Channel-1 trends north, but after meeting with the Alte. Brown SCS, it trends northeast–southwest, deepening and widening down to the BOS. Seaward of Channel-1,

the depositional and erosive features described for the previous sector are also identified in the Valentin Feilberg terrace (Fig. 3). The Ameghino SCS, which lies in the north, has a southern canyon (the largest) with an impressive axial shift: it trends northwest in the upper and middle slopes, northeast at depths of *ca.* 3000–3500 m, and then northwest again, down to the BOS.

The area between the two SCSs (Fig. 3) contains a large sediment wave field at depths of *ca.* 3000–3500 m whose crest has a northeast trend but which otherwise migrates northwest. It contains a submarine terrace at a depth of 3500 m and plastered drifts on the lower slope, at depths of 3500–4500 m, affected by many small valleys created by gravitational processes. The BOS off the Ameghino SCS lacks any rise or large submarine fans, and is closer to the 5000 m isobath than anywhere else in the margin. These features illustrate the dominance of erosive processes at the depths where Channels 1, 2 and 3 merge in the same area, off the Ameghino SCS, and then turn east.

The CDS disappears in the northern zone of Segment II (Fig. 3), because of the dominance of across-slope sedimentary processes. Nevertheless, certain local morphologic features are consistent with the action of Antarctic water masses. These include terraces along the middle slope at depths of *ca.* 1000 m (*Ewing Terrace*) and along the lower slope at a depth of 3500 m (laterally correlated with the Valentin Feilberg terrace); plastered drifts on the lower slope (at depths of 3500–4500 m) affected by erosive features related to the Bahía Blanca SCS; and mixed drifts in the upper rise (at depths of 4500–5000 m) comprising large sediment lobes, whose main axes are oblique (NE/SW) to the general slope trend.

### 5.2. The giant drifts

There are two buried, asymmetrical, mounded and elongated giant contourite drifts in the transition between the base of the slope and the abyssal plain, at 5300–5400 m water depth (Figs. 3–5). Although these were surveyed for the first time in the 1960's by the Lamont Doherty Earth-Observatory, and later by Hinz et al. (1999), they have never before been described. The giant drifts together extend about 250 km, generally south to north (from 47°30' to 45°15'S), southwest of the Cánepa Seamount, which peaks at a water depth of *ca.* 4436 m. El Austral Seamount, which peaks at a water depth of *ca.* 4135 m (Fig. 6A) separates a northern drift from a southern one (hereafter, *northern drift* and *southern drift*, respectively).

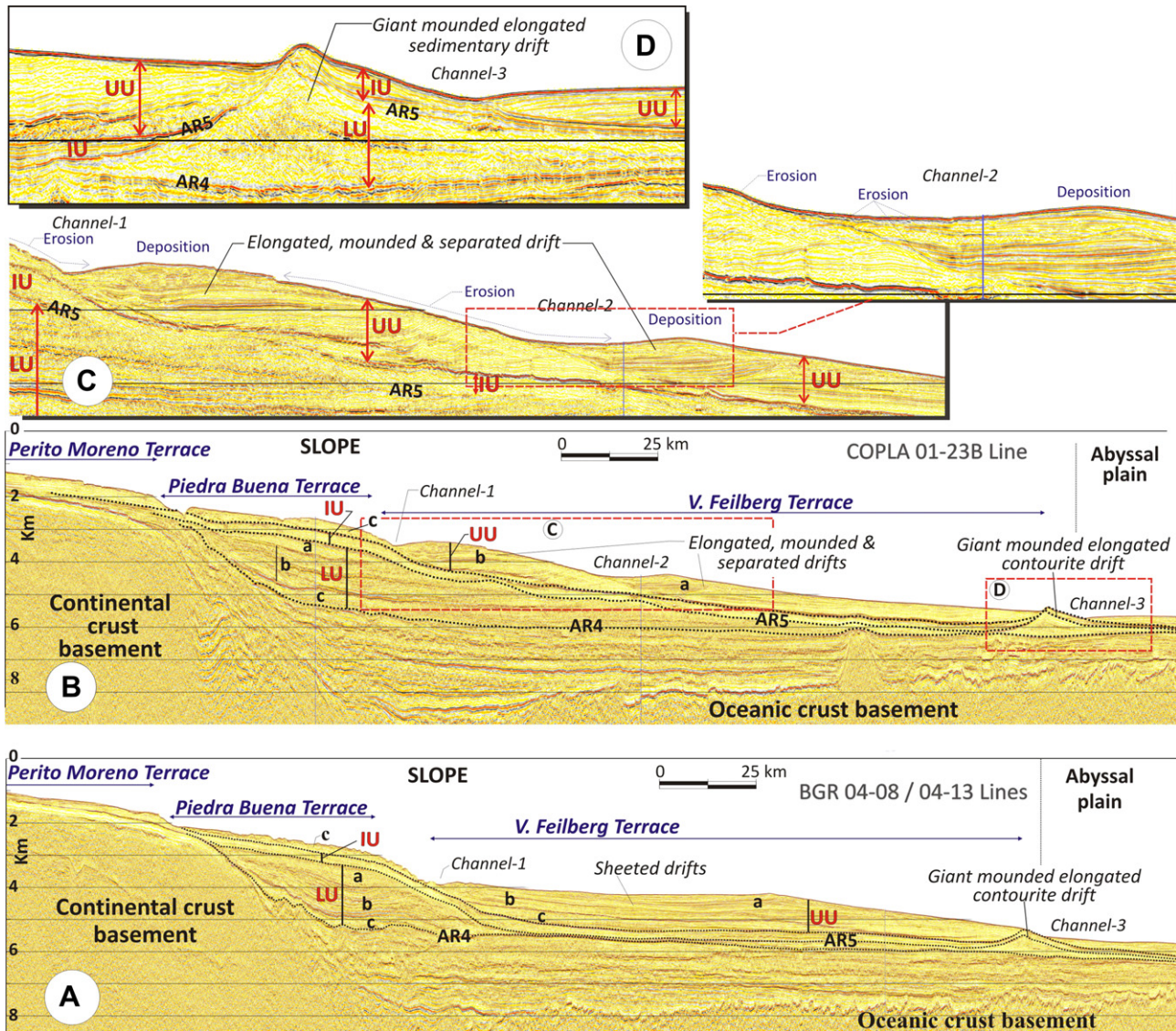


**Fig. 4.** Examples of regional multichannel reflection seismic (MCS) profiles within the Contourite Depositional System at: A) the southernmost part (Lines BGR04-08/04-13); and B) northernmost part (COPLA 01-23b) of the Terrace Sector, with regional stratigraphy framework for the giant drifts. Major morphosedimentary features and seismic units are shown: UU = upper unit; IU = intermediate unit; LU = lower unit; a, b and c are subunits. (C) Close-up figure showing the mounded, elongated and separated drifts and adjacent proximal southern part of the contourite Channels- 1 and 2. (D) Close-up detail of giant drifts. Seismic sections are pre-stack depth migrated.

### 5.2.1. Seismic stratigraphy framework for giant drifts

A regional seismic stratigraphy analysis of the upper part of the sedimentary records of the Argentine CDS was recently performed (see Hernández-Molina et al., 2009). Herein described for the first time is a highly detailed seismic analysis of the giant drifts within the framework of the aforementioned regional study (Fig. 4). Three seismic units have been defined regionally: the Lower Unit (LU), Intermediate Unit (IU) and Upper Unit (UU). The LU is bounded at its base by the AR-4 discontinuity and has moderate to high amplitude reflections that determine lower slope progradation by deposits plastered to the adjacent basement on the lateral slope (Fig. 4 and Table 2). It is internally composed of three subunits (from oldest to youngest: c, b and a). The IU is bounded at its base by the AR-5 discontinuity (Fig. 4 and Table 2). It is an expansive aggradational unit which fossilised the LU and constituted a very good regional stratigraphic level of correlation, due to its overall weak to transparent acoustic response and relatively constant thickness along the entire margin (except for in the buried drifts) (Fig. 4). The present day morphosedimentary features described

above (Fig. 4) began to develop during deposition of the UU, which also comprises three subunits (from oldest to youngest: c, b and a), whose reflections have stratified facies with medium amplitude and good lateral continuity.

The three aforementioned major seismic units can be identified in the sedimentary record where the giant drifts occur. These giant drifts encompass the LU and the IU, and are buried by the UU. The seismic facies of the LU and of the IU differ substantially. The giant drifts are bounded at their base by the AR-4 discontinuity (Hinz et al., 1999), which represents a noteworthy erosional reflection. The giant drifts developed essentially during deposition of the LU, which exhibits the greatest progradation stage and local maximum of thickness (Fig. 4). An important change in the depositional style of drift construction occurred during deposition of the IU: it is characterised by an aggradational stage, but with lateral migration of both the crest drifts and the depocentres (Fig. 4). Although the UU also comprises mounded, elongated drifts and sheeted drifts that remain active, they fossilised the giant drifts developed during the LU and IU, thereby determining a major stage in the style of margin construction.



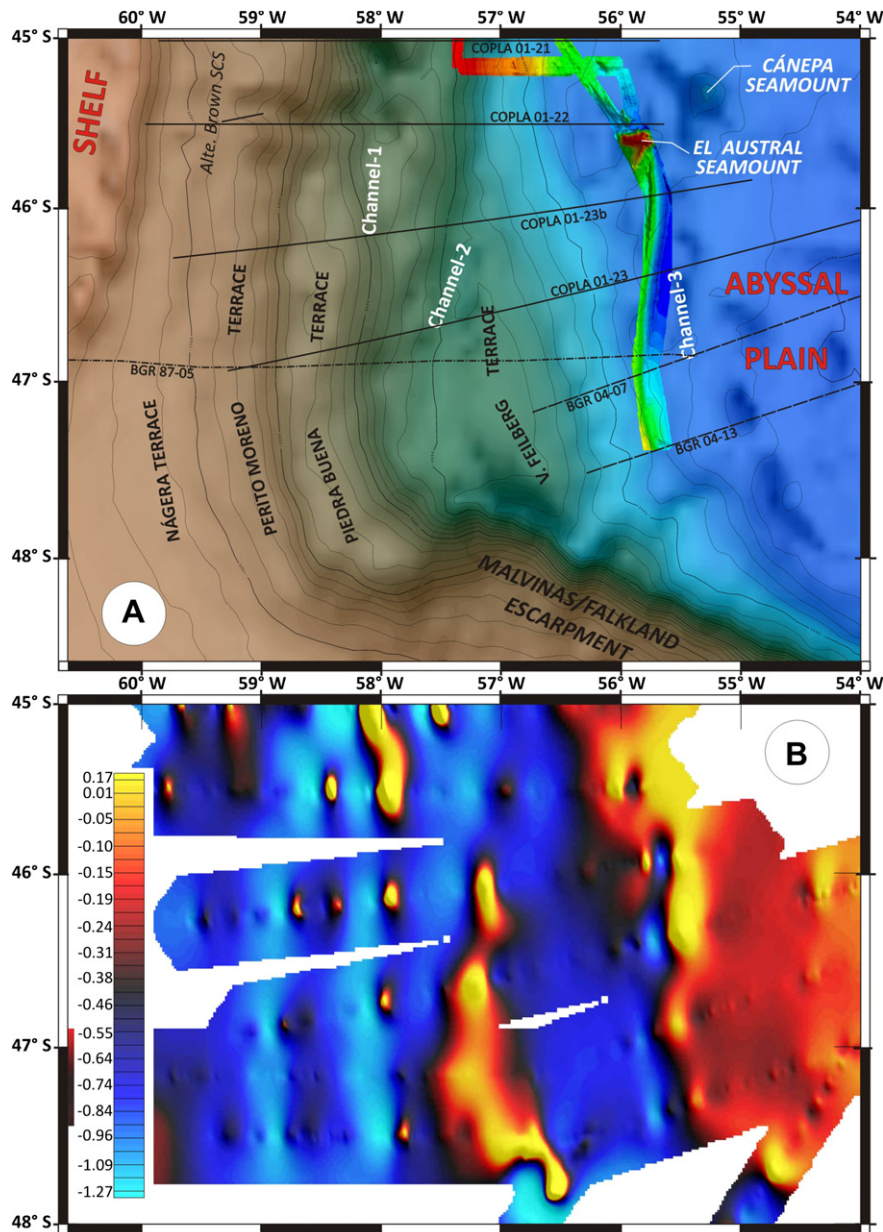


Fig. 5. (A) Bathymetry map with major morphologic elements, showing the location of the swath bathymetric data. (B) Slope gradient map (degree) showing the increase of the base of the slope gradient due to the outcropping of parts of the buried giant drifts.

### 5.2.2. Giant drifts morphology

The giant-drift summits outcrop at present seafloor (Fig. 6A). The summit of the southern drift is shallower close to the El Austral Seamount (5350 m water depth), where a secondary crest (Fig. 6B) deepens southward to 5400 m water depth. The northern drift summit is located at ca. 5450 m water depth, and this drift is separated from the seamount by a narrow, erosive west–east trend channel of 5640 m water depth (Fig. 6A). The drift is fossilised by a thick sedimentary cover from the UU, and had a relief of roughly 400 to 500 m above the adjacent seafloor when they were active (Figs. 6 and 7). Westward of the main crest of the southern drift, the sedimentary cover of UU is ca. 500 m thick (Figs. 6 and 7), establishing the present seafloor at ca. 5400 m water depth. Nevertheless, the sedimentary cover of the UU eastward is thinner (ca. 215 m thick), with a currently erosive seafloor reaching 5700 m water depth along Channel-3. This bathymetric jump on both sides of the

giant-drift crest represents a significant change in the slope gradient trend at the foot of the slope (Fig. 5B).

The giant drifts have different dimensions (Fig. 7). The southern drift is ca. 43 km wide close to the El Austral Seamount (Line 23b), with a slight increase southward (ca. 50 km, Line 23), but it decreases further south, where it reaches a width of 40 km. The sedimentary thickness is higher close to the El Austral Seamount, with a value of 950 m (Line 23b) decreasing toward the south (Fig. 7), where it reaches ca. 830 m (Line 13). The large size and the sedimentary load of the southern drift generate a slight deformation of previous sediments, which is strikingly evident close to the El Austral Seamount, more subdued southward (Lines 23b, 23 and 5), and non-distinguishable in the two southernmost lines (Lines 7 and 13). Local vertical subsidence due to giant-drift occurrence was calculated at ca. 100–150 m (Fig. 7C–E). The local thickness of the Southern drift represents



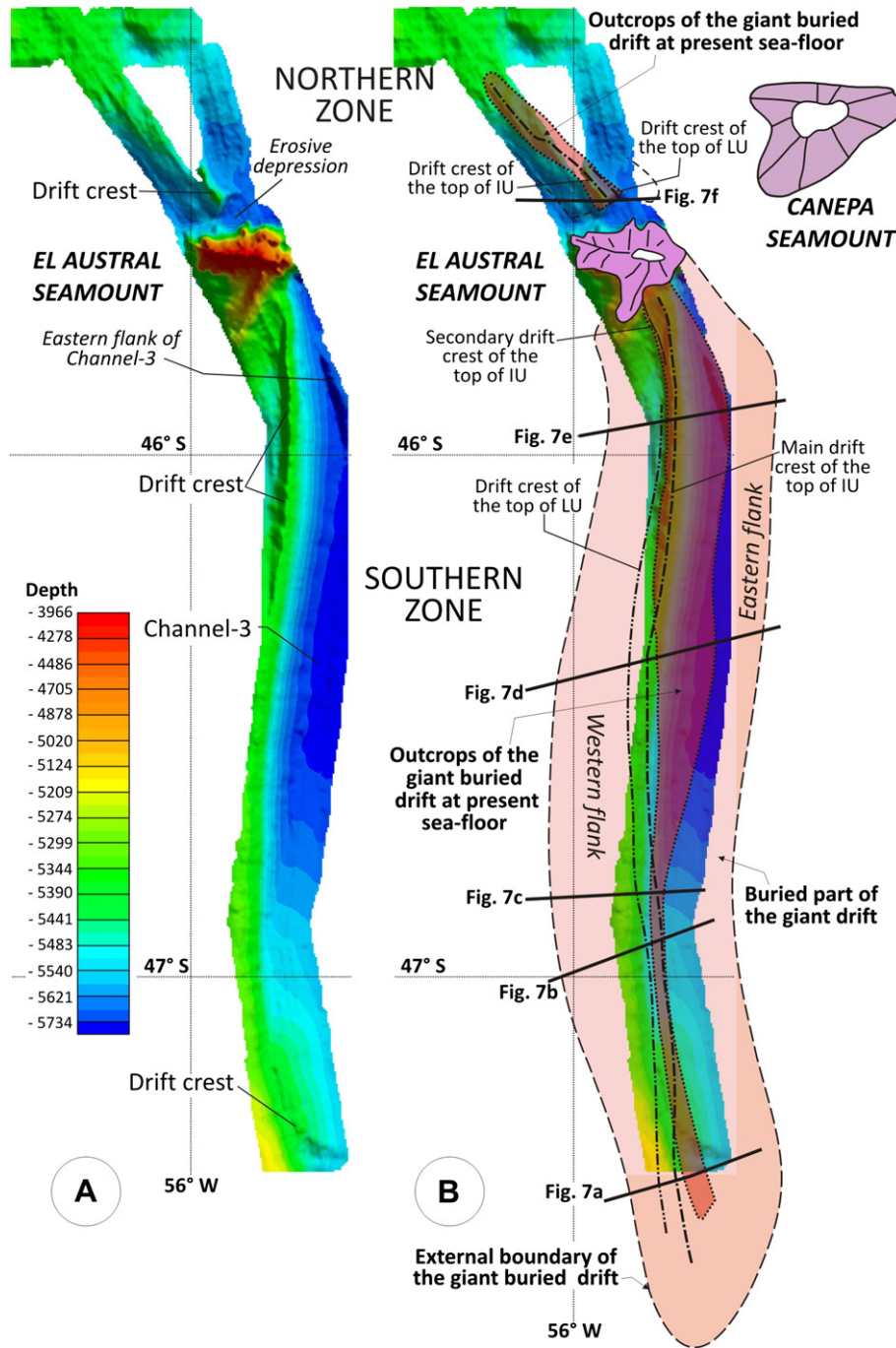


**Fig. 6.** (A) Multibeam bathymetric data collected by the BIO Hesperides (2008), indicating the main present morphologic features around the giant drifts' crests. (B) Sketch showing the positions of the buried giant drifts (with their buried boundaries and the main crests locations associated to the top of the IU and of the LU), and the Cânepa and the El Austral seamounts. The location of the multichannel seismic profiles from Fig. 7 is indicated.

a local gravimetric anomaly in the horizontal gradient: the highest values are associated with the LU rather than with the IU (Fig. 8A). The giant drift gravity model (Fig. 8B) fits very well with the corrected Bouguer anomaly. The sediment covers were assigned a density of up to  $ca. 2.21 \text{ g cm}^{-3}$ . The seismic units within the southern drift are  $1.94 \text{ g cm}^{-3}$  for the LU and  $1.91 \text{ g cm}^{-3}$  for the UU. The corrected Bouguer anomaly (Fig. 8B) reveals bodies that are denser than those of the adjacent environment, which could explain the light load deformation of previous sediments. The asymmetrical external shape of the southern drift is characterised by a steep, west side (on average,

$ca. 1.5\text{--}2^\circ$ ) a gently dipping, smooth east side (on average,  $ca. 0.8$  to  $0.9^\circ$ ) (Fig. 7A–E) that meet to form a long, narrow crest (Fig. 6). The steepest slope ( $ca. 2.1^\circ$ ) is found in the west side of the giant-drift on a line closer to the El Austral Seamount (Line 23b); however, the smoothest slope ( $ca. 0.8^\circ$ ) is located on the east side (Fig. 7E).

In the southern drift, close to the El Austral Seamount (Line 23b) the sedimentary thickness of the LU is  $ca. 800 \text{ m}$ , but toward the south it decreases to  $ca. 600 \text{ m}$ , (Line 13) (Fig. 7A–E). During deposition of the IU, the drift crest shows an eastward and up-gradient migration ( $ca. 1800 \text{ m}$  close to the El Austral Seamount, but  $ca.$



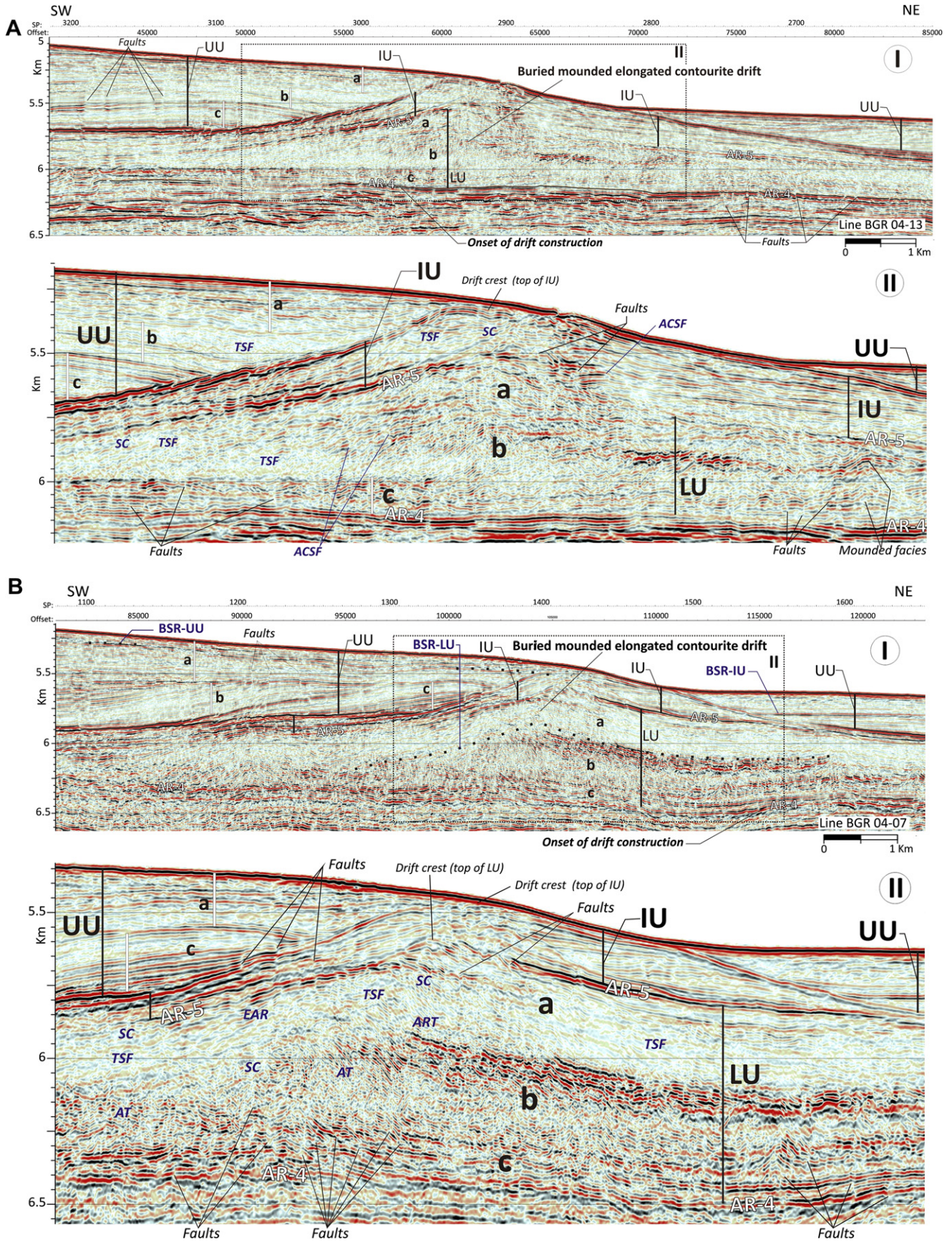


**Fig. 7.** Multichannel seismic reflection profile across the giant drifts, showing major morphosedimentary features, seismic units (LU, IU and UU) and main seismic facies: (A) along the southernmost zone across (Line BGR 04-13); (B, C, D and E) across the giant-drift in the southern zone from south to north until the El Austral Seamount (Lines BGR 04-07; BGR 87-05; COPLA 01-23 and COPLA 01-23b); and (F) along the northern zone after the El Austral Seamount (Line COPLA 01-22). Some examples of seismic evidence of gas hydrates, and of upward migration of free gas and fluids, in the giant drifts are indicated in blue with the following nomenclature: ACSF = Abrupt change in seismic acoustic response or seismic facies; ART = Abrupt reflections terminations; AT = Acoustic turbidity; BSRs = Bottom simulating reflectors; EAR = (local) Enhancement of the amplitude of the reflections; SC = Columnar zone of amplitude reduction (seismic chimneys); TSF = Transparent seismic facies. Profiles location in Fig. 5.



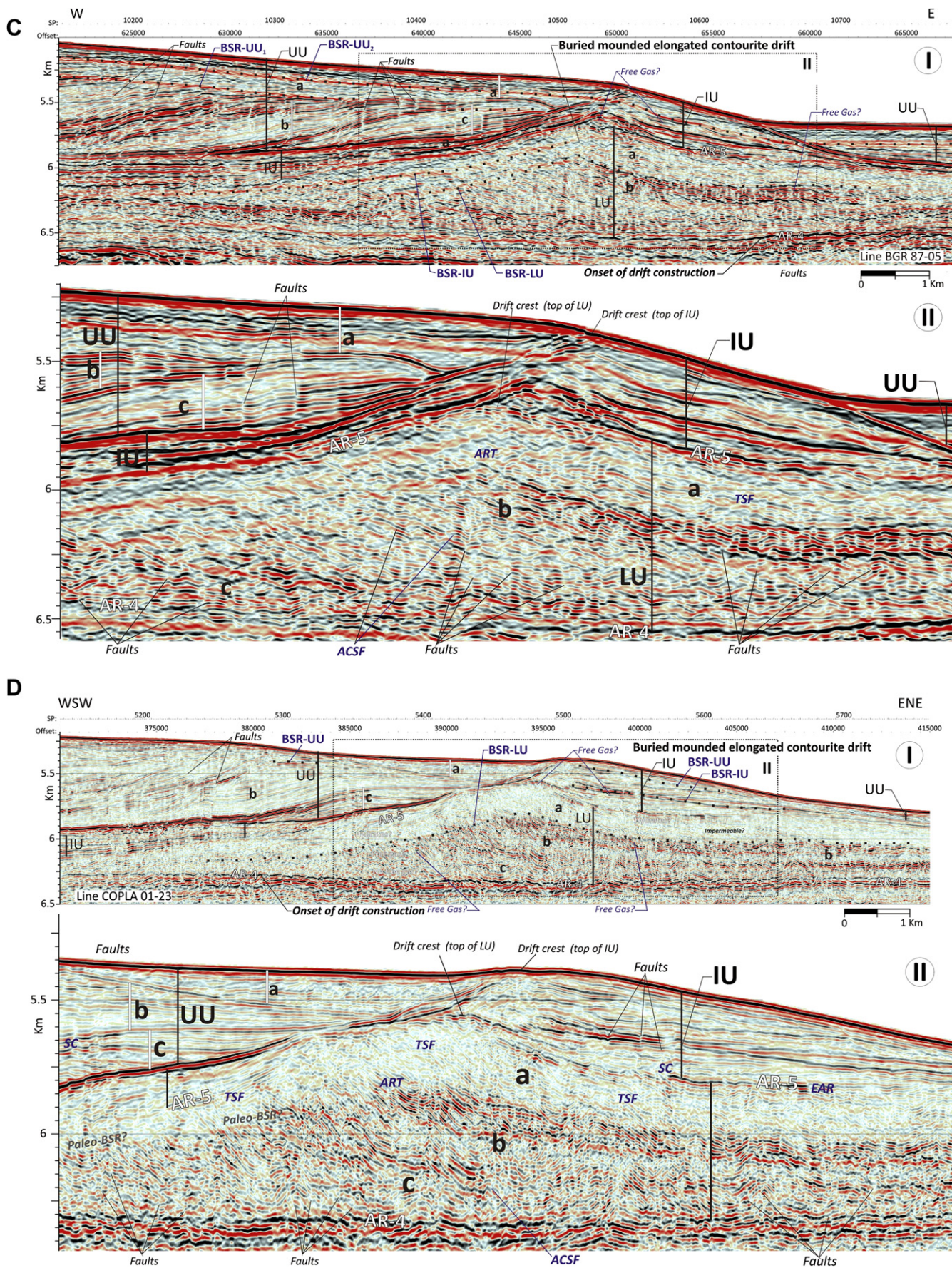


Fig. 7 (continued)



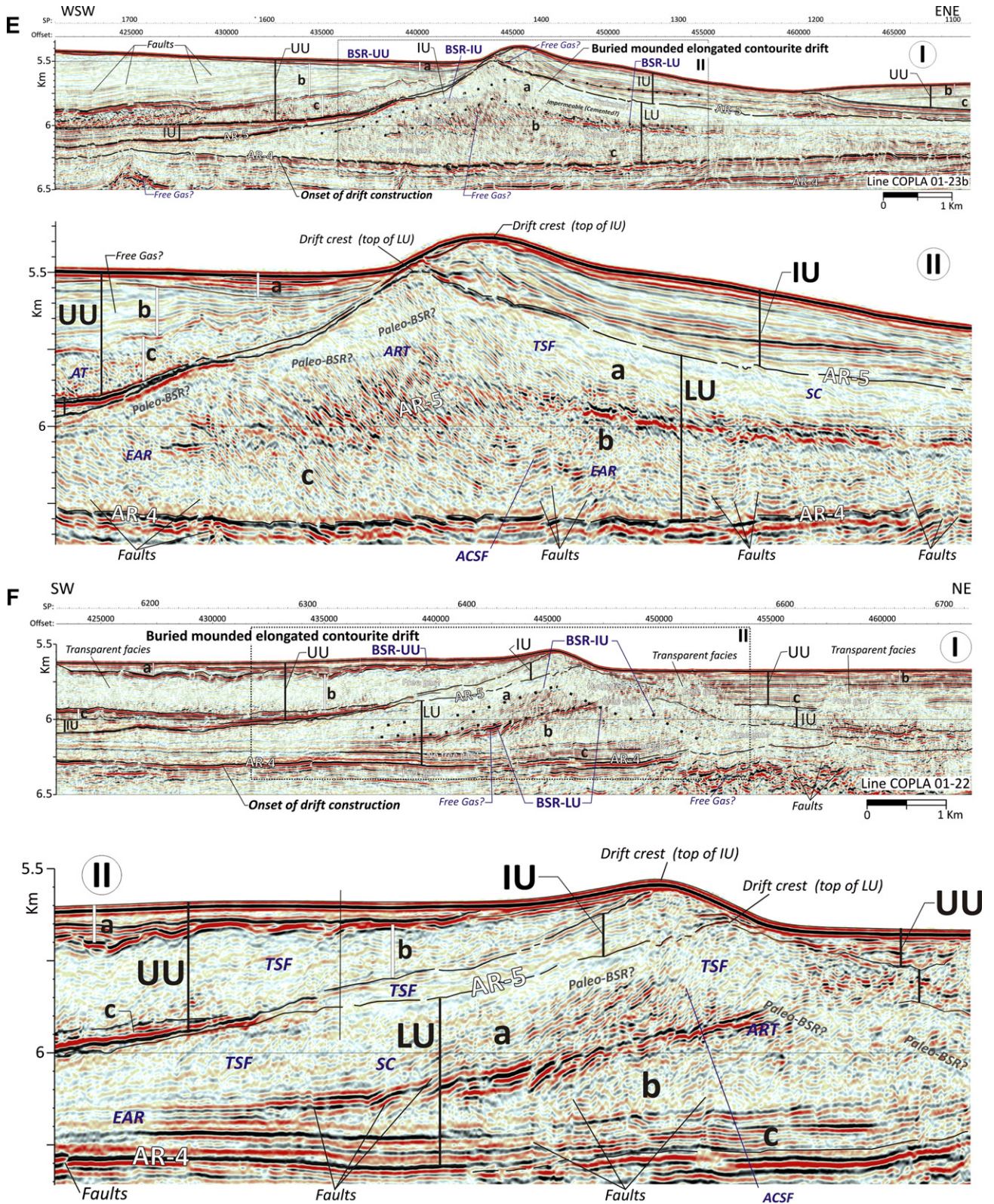


Fig. 7 (continued)

2500 km toward the south) and an aggradation of relatively constant sedimentary thickness (ca. 300 m).

The northern drift is ca. 35 km wide, with a sedimentary thickness of 767 m, which again produces a light deformation of

previous sediments (Line 22) with a local vertical subsidence of ca. 100 m (Fig. 7F). The giant-drift has the opposite geometry to that in the southern zone, with a steep, east side (ca. 1.7°, on average) and a gently dipping, smooth west side (ca. 1–1.2°, on average) (Fig. 7E).



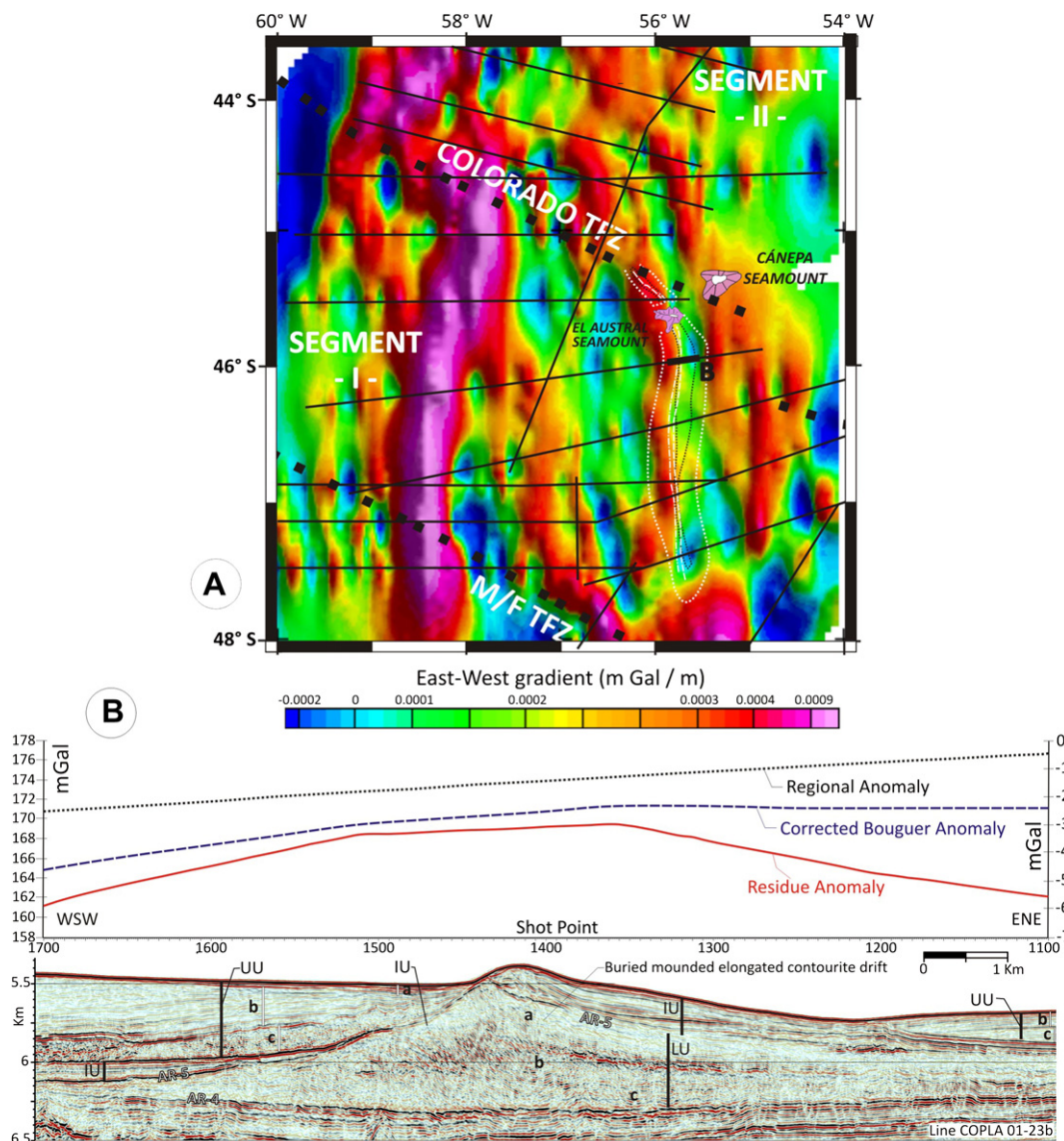


**Fig. 8.** (A) Horizontal gradient map from west to east (for the Segment-I and southern zone of Segment-II) based on the Bouguer Anomalies data. The maximum values on the left are associated to the main sedimentary depocenters of the slope, but a local anomaly was associated to the buried giant drifts occurrence (B). The giant-drift crests associated to the top of the IU and of LU, and buried boundaries, are shown in white lines. The greatest value of these local anomalies was associated to the LU rather than the IU.

The LU has a sedimentary thickness of *ca.* 634 m. The drift crest migrated westward by *ca.* 1.4 km during the IU deposition, which amounts to a thickness of *ca.* 100 m (Fig. 7A–E).

### 5.2.3. Seismic facies and signatures of the identified giant drifts

The buried giant drifts have a trademark seismic signature, especially within the LU, where clear reflections are easy to recognise and continue over long distances (Fig. 7A–E). Nevertheless, the giant drifts generally give weak to transparent acoustic responses, with discontinuous reflections and abrupt changes in their acoustic response. Only a few high-to-very high amplitude reflections with greater lateral continuity were recognised. These enable division of the giant-drift LU into the three subtly different subunits (c, b and a) described above. Subunit-c generally has a relatively high acoustic response (e.g. Fig. 7A–C); Subunit-b has a moderate acoustic response, which increases upward (e.g. Fig. 7B, D and E); and Subunit-a consistently has a very weak to transparent acoustic response (Fig. 7A–F). The giant drifts include large-scale cycles of draping deposition and erosion. The drift crests show a large-scale eastward progradation in the southern drift (Fig. 7A–E), and a westward one, in the northern drift

(Fig. 7F). This change in the internal reflections configuration of the giant-drift coincides with the aforementioned external drift morphology (asymmetry) change. Many polygonal fault structures affecting the recent sedimentary record can be identified, most of which are located down to Subunit-b of the UU, but some of which reach the seafloor. These faults are usually normal faults, although inverse faults and flower structures are also present (Fig. 7A–F) and cross the giant drifts.

Within the LU, a peculiar seismic signature was identified. Here, reflections within the LU are frequently vertically displaced relative to the sedimentary record above and below it (e.g. Fig. 7D and E). Individual reflections are sometimes discontinuous and difficult to follow laterally. Thus, these facies were termed *fluidified facies*. The IU has a regional weak acoustic response along the margin (Fig. 4), although it has a moderate response, with some high amplitude reflections, within the giant drifts. Reflections within the IU show a predominantly aggradational stacking pattern relative to the underlying LU, though large-scale progradation (eastward in the southern drift and westward in the northern one) is visible (e.g. Fig. 7A and B).

Other special seismic signatures were identified within the giant drifts. These include three reflections, crossing the internal reflectors of the LU, IU and UU, whose trend mimicks that of the top of their respective unit (running almost parallel, but 300 m deeper). In fact, there is one reflection in the LU, ca. 300 m below the top of AR5; one in the IU, ca. 300 m below the top of the unit; and one in the UU, ca. 300 m below the present seafloor. These reflections exhibits a phase-reversed reflection relative to that of the seafloor, and their seismic signatures are similar to those of Bottom Simulating Reflectors (BSR) in other areas below present seafloors (Henriet and Mienert, 1998; Pecher and Holbrook, 2000; Chand and Minshull, 2003; Horozal et al., 2008; Løseth et al., 2009).

Other unique seismic signatures comprise abrupt changes in seismic acoustic response; local transparent facies; local enhancement of the amplitude of the reflections; columnar zones of amplitude reduction (defined as *seismic chimneys* or *vertical seismic wipe-outs*); abrupt terminations in reflections; seeps; and acoustic turbidity (Fig. 7C–F). These seismic signatures are strong seismic indicators of gas hydrates, free gas, and upward migration of fluid and gas, as has been considered by many other authors (e.g. Henriet and Mienert, 1998; Pecher and Holbrook, 2000; Vanneste et al., 2002; Chand and Minshull, 2003; Horozal et al., 2008; Løseth et al., 2009). Though a detailed description of these signatures is beyond the scope of this work, it is important to recognise the hydrocarbon potential of the buried giant drift. This could be common in the Argentine Basin, given that similar evidence was earlier discovered in other sectors of the slope (Schümann, 2002; Schümann et al., 2002; Figueroa et al., 2005) and in the abyssal plain (Manley and Flood, 1989).

## 6. Discussion

The evolution and present morphology of the extensional Argentine Margin, particularly of its contourite depositional system (CDS), are the result of Antarctic bottom waters flowing along this margin from the Eocene-Oligocene Boundary (Hernández-Molina et al., 2009). These flows meet through different paths and depths at the southern end of Segment I of the margin, generating the erosive and depositional features of the CDS. The buried, asymmetrical giant-drifts at the base of the slope have not been active from the top boundary of the IU. Their external geometry, internal configuration and evolutionary stages have been deduced by seismic stratigraphy analysis, generating several important points for discussion.

### 6.1. Giant drifts morphologies and their large-scale hydrodynamic consequences

Large, asymmetric isolated mounded drifts are common in deep marine environments. In fact, very large drifts have been described in locations such as the Weddel and Scotia Seas, Antarctica (Maldonado et al., 2003, 2005, 2006), the Greenland margin (Chough and Hesse, 1985; Arthur et al., 1989; Hunter et al., 2007) and the Indian Ocean (Niemi et al., 2000; Uenzelmann-Neben, 2001, 2002; Schlüter and Uenzelmann-Neben, 2007, 2008) and are included in present drift classifications (Stow et al., 2002a; Rebesco, 2005; Rebesco and Camerlenghi, 2008). On the Argentine abyssal plain, at least three huge drifts (Zapiola, Argyro and Ewing) have been identified at the present seafloor (Ewing and Lonardi, 1971; Flood and Shor, 1988).

The Eirik and Agulhas drifts are generated in open, deep marine environments in the northern and southern hemispheres, respectively. Although they differ markedly, they are good examples for understanding formation of the Argentine buried giant drifts. The Eirik drift is connected to the lower slope and rises off the southern tip of the Greenland margin at depths of 1500–3500 m. It is ca.

800 km long and results from the influence of the North Atlantic Deep Western Boundary Current and high sediment input (Chough and Hesse, 1985; Arthur et al., 1989; Hunter et al., 2007). The Agulhas Drift is located in the Transkei Basin (Indian Ocean) at water depths of 4000–4500 m. It extends 350 km in a general east–west direction, and is generated by the influence of the AABW (Niemi et al., 2000; Schlüter and Uenzelmann-Neben, 2007, 2008). The main phase of drift construction started during the lower Pliocene, as a result of the marked increase in thermohaline circulation (Niemi et al., 2000; Hunter et al., 2007; Schlüter and Uenzelmann-Neben, 2008). Both large drifts feature a mounded external shape and asymmetric geometry, with erosion on the steep side and continuous deposition onto the gentler side of the drift, which is typically partly covered with sediment waves. These drifts are located laterally to their respective main core currents: on the right side, in the Eirik Drift (northern hemisphere); and on the left side, in the Agulhas Drift (southern hemisphere) (Niemi et al., 2000; Hunter et al., 2007). External geometry is critical in the construction of these large drifts in deep, open oceans. Migration of the core current in response to the Coriolis Effects determines sediment progradation, and consequently, crest migration, in repeated cycles of drape deposition and erosion (Niemi et al., 2000; Schlüter and Uenzelmann-Neben, 2007, 2008; Hunter et al., 2007; Hunter, 2008). Such migration of the current and of the crest is rightward down-current in the northern hemisphere and the opposite in the southern hemisphere. Nevertheless, mounded drifts in open, deep marine environments differ from those in continental slopes, in which the core current migration is not confined by the slope physiography, and therefore, there is no resulting erosion of sediment and drift construction on the opposite side (e.g. Llave et al., 2001, 2007; Carter and McCave, 2002; Stow et al., 2002b; Carter et al., 2004; Maldonado et al., 2005).

The Argentine giant drifts were generated in an open, deep marine environment. The external morphology of the Southern Drift is characterised by a steep western side and a gently dipping, smooth eastern side with internal reflections that prograde eastward. This asymmetrical morphology was generated by erosion of the western side by periodic, invigorated, bottom-water currents. This suggests that the main core current location that produced the giant-drift in Segment-I, south of the El Austral Seamount, was flowing south, and consequently, the drift grew on the left side down-current (Fig. 9), as occurs in other areas in southern oceans (Niemi et al., 2000; Uenzelmann-Neben, 2001, 2002; Schlüter and Uenzelmann-Neben, 2007, 2008). This interpretation has important regional implications in palaeo-current reconstructions, since the AABW currently flows northward in the same area (Piola and Matano, 2001; Arhan et al., 2002a,b; Hernández-Molina et al., 2009). Therefore, an important regional palaeoceanographic change occurred when the giant-drift became inactive (at the top of the IU). Northward of the El Austral Seamount, the external geometry and internal reflection configuration are opposite to those in the southern zone. Consequently, it can be inferred that when the giant drift was active here, the AABW flowed northward, as it does today (Fig. 9A).

Based on these interpretations, a new regional hydrodynamic model is herein proposed (Fig. 9). During giant-drift deposition, the AABW should flow westwards, passing the Malvinas/Falkland Escarpment until it turns to the north at the Argentine continental slope. Along Segment-I the AABW represents an intensified western boundary current, partially eroding the base of the slope up to the Colorado Transfer Zone location. During the giant-drift deposition, the Argentine Basin was smaller than it currently is and the Colorado Transfer Zone must have been a dominant physiographic feature in the sea floor, because the oceanic crust in Segment-I is older and denser than in Segment-II (Hinz et al., 1999; Franke et al., 2007). One branch of the AABW should turn back



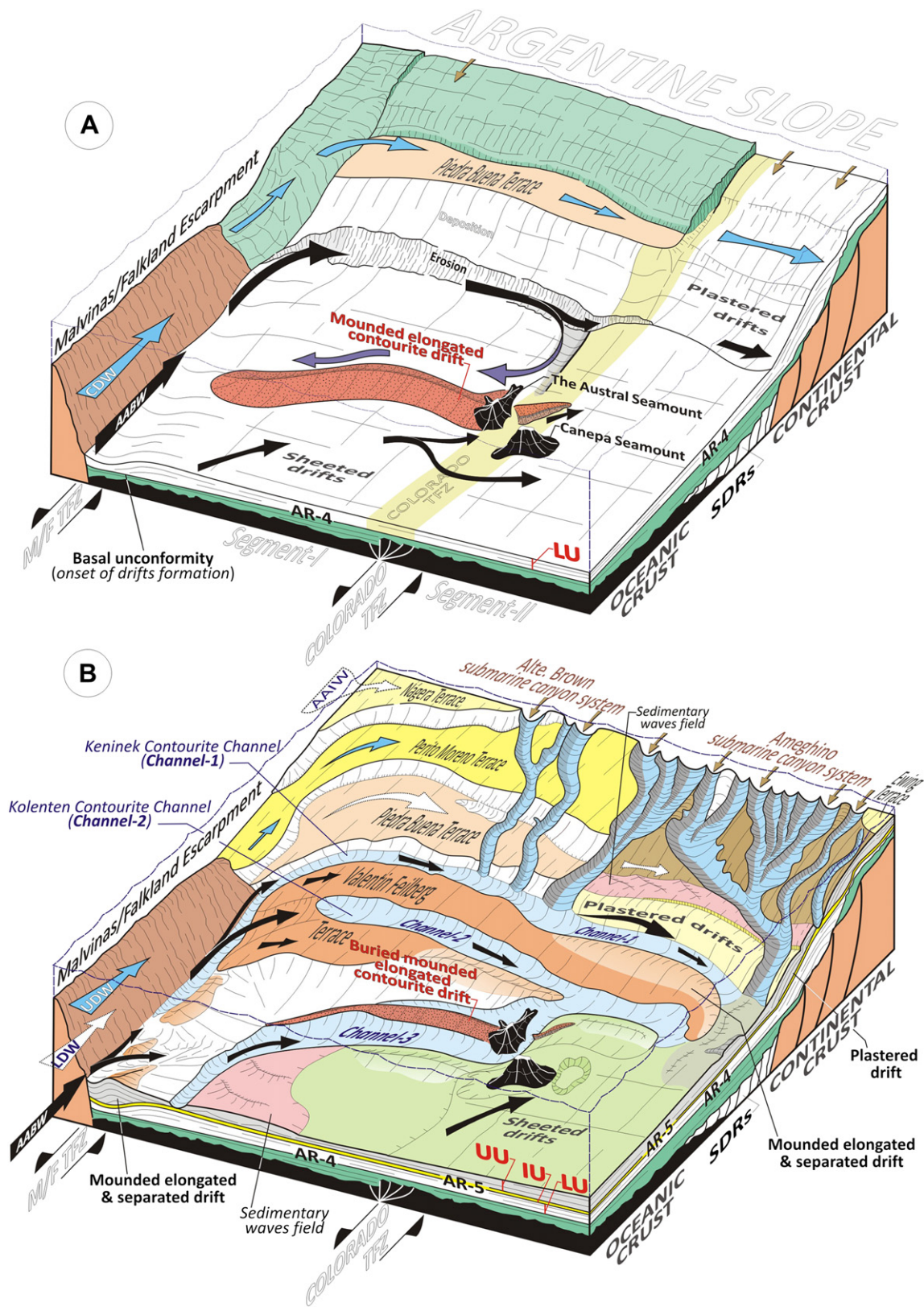


**Fig. 9.** Evolutionary sketches for: (A) development of the giant drifts (LU) and (B) the present scenario. Major tectonic and morphosedimentary features as well as the seismic units and discontinuities are shown. Water masses distribution along the Segment I and southernmost part of Segment II are indicated in every sketch. UU = upper unit; IU = intermediate unit; and LU = lower unit.

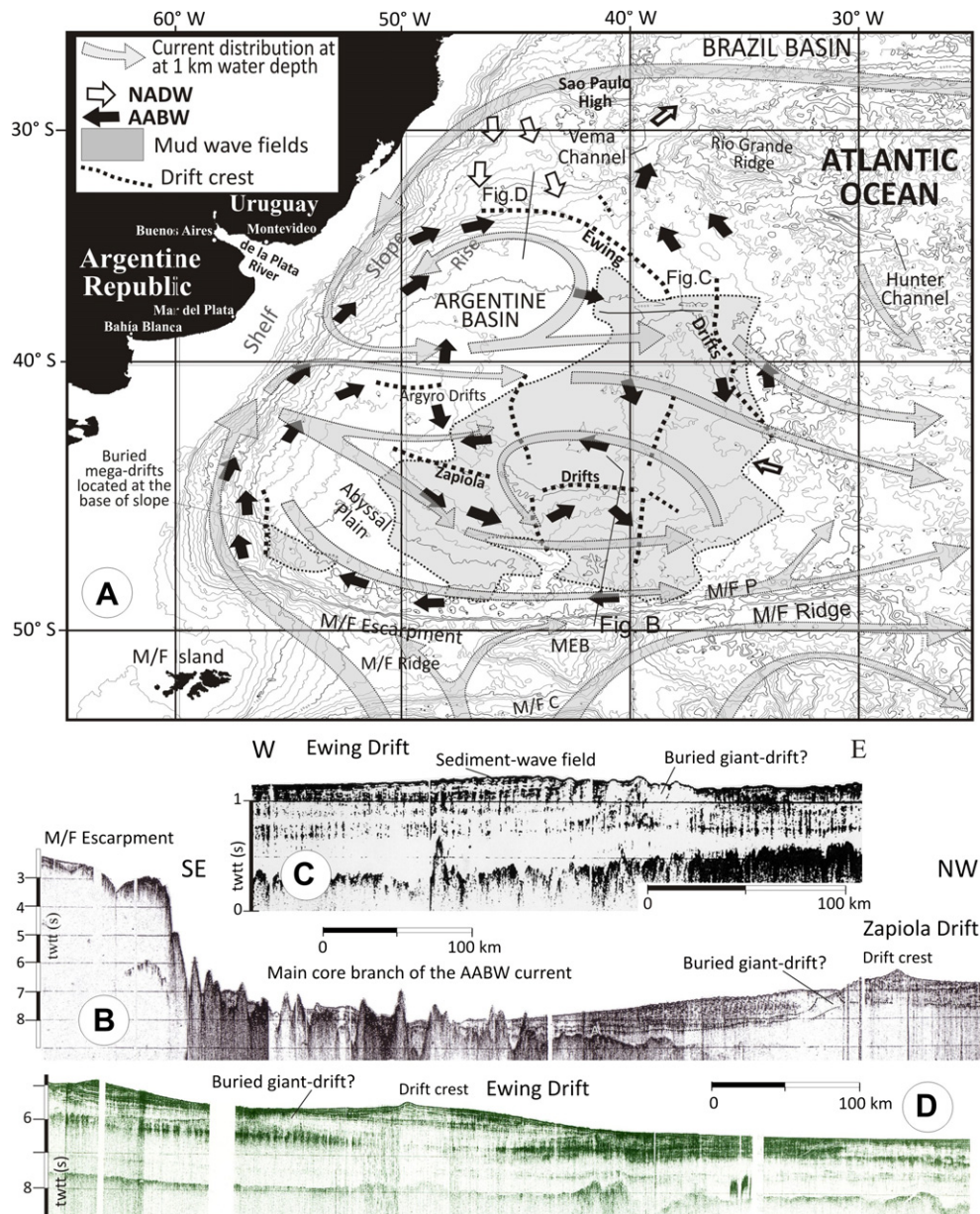


**Fig. 10.** (A) Sketch with regional bathymetric map, general circulation of intermediate and deep water masses (AABW and NADW), and the position of the three large contourite drifts (Zapiola, Argyro and Ewing Drifts) in the Argentine Basin (compilation using data from: Flood and Shor, 1988; Speer et al., 1992; Reid, 1989, 1996; Klaus and Ledbetter, 1988; Boebel et al., 1999). Intermediate circulation of water masses has been greatly simplified; for further details, see Boebel et al. (1999). (B) Profile across the Zapiola drift and the Malvinas/Falkland Escarpment (data courtesy of the Argentine Navy Hydrographic Service, Argentina). On B, we have included the original interpretation of Le Pichon et al., 1971. (C and D) Sheeted and mounded deposits of the Ewing Drift. Seismic profile on C from Barker et al. (1976) and from D courtesy of the Argentine Navy Hydrographic Service, Argentina. Note that both the Zapiola and the Ewing drifts should have large, buried contourite deposits. Also note the similitude between the north trend of the crests of the Zapiola and the Ewing drifts with the trend of the buried giant-drift crest located in the base of the slope.

toward the south, forming a huge loop at the end of Segment-I and generating depositional processes beyond the El Austral Seamount, which represents an isolated obstacle to the flow (Fig. 9A). At the beginning of Segment-II, beyond the Colorado Transfer Zone, the AABW should flow northward (Fig. 9A).

Various sediment inputs to generation of giant drifts should be considered, a concept recently proposed by Stow et al. (2008). Pelagic-hemipelagic (which come from multiple sources) turbidity currents from adjacent slopes, and bottom currents with local erosion and longer-distance transport, could act as sediment inputs for construction of giant drifts. Active and generally stable bottom currents serve to focus sedimentation in the open deep ocean, and therefore, build up drifts over very long periods of time, especially in

the lee of large submarine obstacles (Hernández-Molina et al., 2006). Drift development is enhanced by external factors that promote deposition rather than simple transport, including (Stow et al., 2008): excess concentration and/or grain size due to current interaction, high surface productivity, local erosion around obstacles, distal input from terrestrial sources, etc.; and topographic effects such as obstacles to flow, changes in bottom-current pathway, and subtle changes in bottom gradient. Open ocean pelagic sediment is thereby focused to present variable thicknesses of accumulation over long periods of time, rather than the uniformly thick sediment blanket generally associated with deep oceans (Stow et al., 2008). Moreover, sediment from the continent could reach the deep ocean through stratified nepheloid layers. Sediment entrained in the



nepheloid layers can be deposited by currents decelerated by isolated obstacles and by outflowing at the outer curve of oceanic loops (Niemi et al., 2000; Hernández-Molina et al., 2006; Stow et al., 2008).

Flowing of AABW over a long period of time along the Argentine slope (in the LU and the IU) may have focused deposition in the lee of the El Austral Seamount, consequently generating the giant drift (Fig. 9). El Austral Seamount represented a punctual obstacle that conditioned the formation of a relatively stable core of the main AABW southward, whereby the giant drift is located laterally and to the left (*i.e.* downcurrent). Depositional processes are favoured due to the generation of a shadow zone, downstream of the seamount, where flow intensity diminishes slowly. At the outer bend of the south-to-southwest directed AABW, current along the 5300–5400 m isobaths sediments should be deposited as drapes, forming the giant drift (Fig. 9A), similarly to the scenario proposed by Niemi et al. (2000) for the Agulhas Drift. The lower level of lateral migration during deposition of the IU close to the El Austral Seamount compared to that in the distal, southern part of the giant-drift, results from the fact that the seamount constituted a fixed obstacle feature, and consequently, minor possible changes in direction of the impinging flow must have affected the distal part of the drift to a much greater extent than it did the area close to the obstacle. Furthermore, high amplitude internal reflections within the giant-drift sedimentary architecture should indicate large-scale changes in bottom current strength, and therefore, alternating periods of deposition and erosion from the AR4 discontinuity to the top of the IU, similarly to what was described in the Eirik and Agulhas drifts (Niemi et al., 2000; Uenzelmann-Neben, 2001, 2002; Schlüter and Uenzelmann-Neben, 2007, 2008 Hunter et al., 2007).

Although the present location of the three huge drifts on the Argentine abyssal plain (Zapiola, Argyro and Ewing drifts, Fig. 1) has been described, as has their genesis, which is associated to the long-term cyclonic movement of AABW (Ewing and Lonardi, 1971; Flood and Shor, 1988), no work regarding their onset, internal structure or evolution has yet been published. Therefore, any comparison between the described buried giant-drift and the aforementioned present abyssal plain drifts would be rather speculative. Nevertheless, these features share an intriguing degree of similitude in drift crest trend. The Zapiola drifts have a giant, flat-lying letter “H”, with two drift crests trending north and one crest trending east to southeast (Figs. 1 and 10). The Ewing drifts are divided into two zones: a western one, in which the drift crest has an east to southeast trend, and an eastern one, in which the drift crest trends south-southeast. The Argyro Drifts have a drift crest with an easterly trend. The chiefly northerly trend of the buried giant drifts is roughly parallel to the northerly trend of the crests in the Zapiola Drifts and the eastern part of the Ewing Drifts. The Zapiola Drift is roughly equal in length to the buried giant-drift (*ca.* 350 km), but it is higher above the adjacent seafloor (*ca.* 1200 m). The northerly trend of the crests in the Zapiola Drifts is somewhat perpendicular to the present regional hydrodynamics model (Fig. 10A) at basin scale for both intermediate (Boebel et al., 1999) and deep-water circulation (Flood and Shor, 1988; Reid, 1989, 1996; Klaus and Ledbetter, 1988; Speer et al., 1992; Faugères et al., 1993; Piola and Rivas, 1997; Piola and Matano, 2001). Nevertheless, the west–east trends of the crests in the Zapiola and Argyro Drifts, which are almost perpendicular to the buried giant-drift (Fig. 10A), are fully coincident with the present hydrodynamics model at basin scale for both the present intermediate and deep water circulations (cited references). Another similarity between the buried giant drifts and the Zapiola Drifts is that from the single-channel seismic reflection profiles collected by the Lamont-Doherty Earth Observatory, both the Zapiola and Ewing Drifts seem to have giant drifts partially buried by a recent, thicker, sedimentary cover that defines a different stage in drift construction and that is associated with the present west–east drift crests

(Fig. 10). This tentative comparison could support the following scenario, proposed here for the first time: that the aforementioned palaeoceanographic change occurred at basin scale.

## 6.2. Evolutionary stages of giant drift constructions, and their palaeoceanographic implications

Based upon the stratigraphic analysis, three stages in the giant drifts evolution should be considered.

### 6.2.1. Growth stage (LU)

This stage started with development of the AR4 discontinuity and developed further during LU deposition. The AR4 discontinuity represents the onset of AABW circulation in the Argentine Basin and contourite deposition. Hinz et al. (1999) dated this discontinuity to the Eocene-Oligocene boundary, which could be related to opening of the Drake Passage (*ca.* 32–31 Ma), when it was deep enough for deep circulation (Livermore et al., 1994, 2004; Barker, 2001; Lawver and Gahagan, 2003; Lagabriele et al., 2009). The AR4 discontinuity is correlated with AR-I unconformity from Urien et al. (1976), and related to the Horizon B defined in the northeast of the Argentine Basin at site DSDP-358 (Ewing and Lonardi, 1971), which marks an important change in sediment facies (Supko and Perch-Nielsen, 1977). The AR4 discontinuity is coeval with the R1/D2 discontinuity in the Brazil Basin (Mézerai, 1991; Mézerai et al., 1993; Lima, 2003; Viana et al., 2003), Discontinuity O in the Indian Ocean (Niemi et al., 2000) – which is coincident with a regional hiatus in the sedimentation (Latimer and Phillipelli, 2002) – and the Marshall Paraconformity in the South Pacific Ocean (Carter et al., 2004). The AR4 discontinuity could also be associated with the extension of ice in East Antarctica (Barron et al., 1989; Cooper et al., 1991) and the beginning of a new THC system that affects the south hemisphere (Supko and Perch-Nielsen, 1977; Kennett, 1982).

During this interval, the AABW was an intensified western boundary current in the Argentine margin, partially eroding the base of the slope along Segment-I, to later form a huge loop, spanning from the end of this Segment to the Colorado Transfer Zone location (Fig. 9A). One branch of the AABW should have turned back southward, generating deposits south of the El Austral Seamount, which would represent an isolated obstacle to this branch. Under this scenario, the giant drift would have developed as a large, asymmetrical elongated and mounded sedimentary body (Fig. 9A).

Part of this interval is coeval with the progressive constriction of the Drake Passage, which occurred from 21 to 15 Ma (Lagabriele et al., 2009) and which could have gradually accelerated the dynamics of Antarctic water masses due to progressive reduction of the passage section. Also, throughout most of this interval, both the Hunter and Vema channels were too shallow to allow a deep connection between the Argentine and Brazil Basins; indeed, this connection arose in the lower Miocene (Kennett, 1982). All these features have contributed to a hydrodynamic circulation model for the AABW within the Argentine Basin.

### 6.2.2. Vertical growth stage (IU)

This stage began from the AR5 discontinuity and developed further during IU deposition. The AR5 discontinuity was dated by Hinz et al. (1999) to the early middle Miocene (*ca.* 15 Ma), which is coeval with Discontinuity M in the Indian Ocean (Niemi et al., 2000), and an unconformity in the South Pacific Ocean (Carter et al., 2004). Several important events occurred in southern South America after 15 Ma, coeval with the re-opening and deepening of the Drake Passage, after 15 Ma (Lagabriele et al., 2009): first, the margin underwent a massive aggradational phase, which could be

associated with major regional subsidence and global third-order highstand intervals in the middle Miocene (Van Andel et al., 1977; Kennett, 1982; Haq et al., 1987; Malumian and Olivero, 2005); second, the end of the compressional tectonics in the Patagonian Cordillera (Barreda and Palamarczuk, 2000); third, a marked rise in sea level over the South American continent (Aceñolaza, 2000); and last, widening of the Drake Passage due to active oceanic spreading along the Phoenix-Antarctic Ridge, from 15 to 8–3 Ma (Livermore et al., 2000; Eagles, 2003), and along the East Scotia Ridge, since 20 Ma (Eagles et al., 2005).

Despite the general sedimentary model proposed for deposition of the LU, the giant-drift had its main vertical growth interval during this stage. However, the axis of the crest during this stage is shifted by several hundred meters eastward, south of the El Austral Seamount, and westward, north of this seamount. This indicates a minor change in current direction, which could be coeval with the fact that at 15 Ma, bottom-current activity due to AABW was mainly restricted to depths below ca. 5.5 km (Sykes et al., 1998).

### 6.2.3. Inactive stage (UU)

The giant-drifts became inactive during this stage (Fig. 9B) which began from the base of UU, marking the start of major changes in palaeoceanography and depositional type at the basin scale that led to partial burying of the giant drifts. Palaeoceanographic changes implied more vigorous intermediate and deep circulation after deposition of the IU. These changes ended after formation of Subunit-c of the UU, when a new oceanographic scenario was completely established and present morphologic features began to develop (Hernández-Molina et al., 2009). The base of the UU could date to the late middle Miocene (Hinz et al., 1999), which is coeval with the R2/R4/D4 discontinuity in the Brazil Basin (Mézerai, 1991; Mézerai et al., 1993; Lima, 2003; Viana et al., 2003), and Reflector-c in the Weddell and Scotia Seas in Antarctica (Maldonado et al., 2006).

There is evidence for a coeval Middle Miocene increase in the deep-water circulation in the Southern Hemisphere (Kennett, 1982; Carter et al., 2004; Joseph et al., 2004), with good examples in the northern Weddell and Scotia Seas (Maldonado et al., 2006), and in the rise of the Pacific margin of the Antarctic Peninsula (Rebesco et al., 2002). Increased water-mass circulation could correlate to the middle Miocene event coeval with a major Miocene glaciation (Mi4), a sea-level lowering (Ser3), the initiation of the permanent eastern Antarctic ice-sheet, and/or with the initiation of NADW circulation in the southern hemisphere (Kennett, 1982).

The palaeoceanographic change that generated a new oceanographic scenario to fossilise the giant-drift (Fig. 9B) could be related to the middle Miocene initiation of NADW circulation in the Atlantic and its Lower Pliocene enhancement (Hernández-Molina et al., 2009). During the late middle Miocene, NADW began to circulate, and then extended into the Southern Hemisphere (Kennett, 1982). Concurrently, the Central American Seaway (CAS) was deeper than the level of NADW outflow (Nisancioglu et al., 2003); therefore, a significant amount of NADW passed through the CAS into the Pacific Ocean, reducing the potential amount of NADW transported to the South Atlantic. In the Pacific, NADW became a southward flowing, western boundary current, before it joined with the ACC to the south (Nisancioglu et al., 2003). LCDW derives from NADW and, therefore, has existed since the middle Miocene, when the CDW started to split into two fractions (UCDW and LCDW), the ultimate consequences of which, for the Argentine Basin, should have been the onset of LCDW circulation and the deepening of the CDW-AABW interface (Hernández-Molina et al., 2009). Although these changes should have begun after the base of UU, a more dramatic change occurred in association with the reflection at the top of Subunit c of UU, which has been correlated

with R4'/R3/top of U2c discontinuity in the Brazil Basin (Mézerai, 1991; Mézerai et al., 1993; Lima, 2003; Viana et al., 2003); Discontinuity P in the Indian Ocean (Niemi et al., 2000); an unconformity in the South Pacific Ocean (Carter et al., 2004); a hiatus in the Southern Ocean (Ledbetter and Ciesielski, 1986); and Reflector-b in Antarctica (Maldonado et al., 2006). Therefore, the reflection could date to late Miocene/early Lower Pliocene, for which there is major evidence of relatively strong activity in the intermediate and deep-water circulations (Sykes et al., 1998). Given that the CAS shoaled at that time, the NADW could not flow into the Pacific, but its flow to the South Atlantic did increase, creating a more vigorous water circulation pattern (Nisancioglu et al., 2003). This change would be associated with ocean bottom cooling due to the expansion of western Antarctic ice-sheet and fringing ice-shelves (Ledbetter and Ciesielski, 1986; Niemi et al., 2000; Anderson and Shipp, 2001), and the initiation of ephemeral Northern Hemisphere ice sheet, coincident with a global temperature drop (Jansen and Raymo, 1996). Consequently, the Antarctic water masses also expanded with major implications for Argentine margin Segments I and II, where the present morphosedimentary features of the CDS began to form along the Argentine slope, and depositional processes were favoured at depths greater than 3500 m, which partially fossilised the giant-drift (Fig. 9B). The new basin oceanographic scenario after Subunit c deposition could be also partly due to the fact that throughout the Lower Pliocene, the Vema channel was deep enough for AABW circulation (Kennett, 1982), which in turn could have caused major internal hydrological changes in the basin circulation.

## 7. Conclusions

Buried, asymmetrical, mounded, elongated contourite drifts are located in the southernmost sector of the extensional Argentine margin, below the presently active Contourite Depositional System (CDS). These feature a northerly trend at the base of the slope, at water depths of 5300–5400 m. Their summit outcrops at present seafloor, generating a bathymetric jump that represents an important change in the slope gradient trend at the base of the slope. The following conclusions regarding the giant drifts have been made:

- Giant drifts were generated in an open, deep marine environment. Two major drifts have been identified, south and north of a large seamount (El Austral Seamount): the southern drift and the northern drift.
- The southern drift is ca. 40–50 km wide and 250–300 km long and has a sedimentary thickness of 950–830 m. The asymmetrical external shape is characterised by a steep west side and a gently-dipping, smooth east side. Local internal reflections prograde eastward. In contrast, the northern drift is ca. 35 km wide and has a sedimentary thickness of 767 m. Its geometry is opposite to that of the southern zone: its west side is smooth and its east side is steep. Likewise, its internal reflections prograde westward.
- The seismic facies of the giant drifts shows very weak to transparent acoustic response, with discontinuous reflections and abrupt changes in the acoustic response, indicating a fluidified seismic signature. There are high amplitude reflections with greater lateral continuation (but that are affected by many faults) that reveal that large-scale cycles of drape deposition and erosion have combined to form the giant drifts.
- The southern drift was generated by the southward flow of AABW, which began after the Eocene-Oligocene boundary until middle Miocene.
- The drifts were inferred to record a major palaeoceanographic change between the middle to very late Miocene. Changes in



the regional hydrological model were attributed partly due to the initiation of NADW circulation in the southern hemisphere. The water-mass conditioned the formation of LCDW in Antarctica as well as the deepening of AABW circulation in the Argentine Basin, which has been the major controlling factor of sedimentary processes in the lower slope and abyssal plain from the middle Miocene to present.

- Based on the conclusions above, a new oceanographic scenario was established for the period spanning the middle Miocene to present. This scenario has been imputed in the burial of the giant drifts as well as in generation of a new margin morphology, with development of present day morphosedimentary features of the CDS generated from the northward flow of the Antarctic water masses.
- Strong seismic evidence of gas hydrates and free gas, and of upward migration of gas and fluids, was found within the giant drifts. Thus, these buried giant drifts appear to be rich in possibilities for energy exploration, although this must be confirmed by further study, they could represent a prime example of the economic potential of contourite deposits in deep marine environments.
- The results presented in this paper are testament to how large contourite drifts in deep marine environments can yield evidence for reconstructing palaeoceanographic changes, and help to explain Thermohaline Circulation and climate in the past.

## Acknowledgements

This work has been partially completed during a research stay by F. J. Hernández-Molina at the Marine Geology and Geophysical Division of the Argentine Navy Hydrographic Service, funded by the Mobility Award of the Spanish Ministry of Education and Science (PR2007-0138). This work was also supported by the Spanish Comisión Interministerial de Ciencia y Tecnología (CYCIT) through projects CTM 2008-06399-C04/MAR (CONTOURIBER Project) and CTM2008-06386-C02/ANT. This contribution is also related to the Argentine Project ANPCyT – PICT 2003 N° 07-14417. The authors thank COPLA (Argentina) and the BGR (Germany) for allowing us to use their bathymetric and multichannel seismic (MCS) reflections profiles database. The authors would like to thank Dr. A. Piola (SHN, Argentina) for revision and comments on the oceanography setting, L. Maffía (COPLA, Argentina) for her help in drawing Fig. 3, and Daniel Alberto Abraham (Faculty of Engineering, University of Buenos Aires, Argentina) for calculating the oceanic crust age in the studied area. We thank to K. Hinz for our initial discussions about both the “Frida-Drift” and major geology characteristics of the Argentine margin. Finally, we also thank both Editors and two anonymous reviewers for their interest and suggestions, which have helped us to improve the final version of our manuscript.

## References

- Aceñolaza, F.G., 2000. La Formación Paraná (Mioceno medio): estratigrafía, distribución regional y unidades equivalentes. In: Aceñolaza, F.G., Herbst, R. (Eds.), El Neógeno de Argentina. Serie Correlación Geológica, vol. 14. INSUGEO, Tucumán, pp. 9–27.
- Anderson, J.B., Shipp, S.S., 2001. Evolution of the West Antarctic ice-sheet. In: Alley, R.B., Bindshadler, R.A. (Eds.), The West Antarctic Ice-sheet: Behavior and Environment. Antarctic Research Series, vol. 77. AGU, pp. 45–58.
- Arhan, M., Naveira-Garabato, A., Keywood, K.J., Stevens, D.P., 2002a. The Antarctic Circumpolar Current between the Falkland Islands and South Georgia. *Journal of Physical Oceanography* 32, 194–1931.
- Arhan, M., Carton, X., Piola, A., Zenk, W., 2002b. Deep lenses of circumpolar water in the Argentine Basin. *Journal of Geophysical Research* 107 (No. C1), 3007. doi:10.1029/2001JC000963.
- Arthur, M., Srivastava, S.P., Kamiski, M., Jarrad, R., Osler, J., 1989. Seismic stratigraphy and history of deep circulation and sediment drift development in the Baffin Bay and the Labrador Sea. In: Srivastava, S.P., Arthur, M., Clement, B. (Eds.), *Proceeding of the Ocean Drilling Program, Scientific Results*, vol. 105, pp. 957–988. Ocean Drilling Program, College Station, TX.
- Barker, P.F., 2001. Scotia Sea regional tectonic evolution: implications for mantle flow and palaeocirculation. *Earth-Science Review* 55, 1–39.
- Barker, P., Dalziel, I.W.D., Dinkelman, M.G., Elliot, D.H., Gombos Jr., A.M., Lonardi, A., Plafker, G., Tarney, J., Thompson, R.W., Tjalsma, R.C., von der Borch, C.C., Wise Jr., S.W., 1976. Site 331: Argentine Basin. In: Wise Jr., Sherwood W. (Ed.), *Initial Reports of the Deep Sea Drilling Project*. US Govt. Printing Office, Washington, pp. 259–265.
- Barreda, V., Palamarczuk, S., 2000. Estudio palinoestratigráfico del Oligoceno tardio-Mioceno en secciones de la costa patagónica y plataforma continental argentina. In: Aceñolaza, F.G., Herbst, R. (Eds.), El Neógeno de Argentina. Serie Correlación Geológica, vol. 14. INSUGEO, Tucumán, pp. 103–138.
- Barron, J., Larsen, B., et al., 1989. *Proceeding of the Ocean Drilling Program, Initial Reports*, vol. 119. College Station, TX (Ocean Drilling Program).
- Boebel, O., Davis, R.E., Peterson, R., et al., 1999. The intermediate depth circulation of the western south Atlantic. *Geophysical Research Letter* 26, 3329–3332.
- Carter, L., Carter, R.M., McCave, I.N., 2004. Evolution of the sedimentary system beneath the deep Pacific inflow off eastern New Zealand. *Marine Geology* 205, 9–27.
- Carter, L., McCave, N., 2002. Eastern New Zealand drifts, Miocene–recent. In: Stow, D.A.V., Pudsey, C.J., Howe, J.A., Faugères, J.C., Viana, A.R. (Eds.), *Deep-Water Contourite Systems: Modern Drifts and Ancient Series, Seismic and Sedimentary Characteristics*. Geological Society of London, Memoir 22, 385–407.
- Carter, L., McCave, I.N., Williams, M.J.M., 2009. Circulation and Water Masses of the Southern Ocean: a review. In: Florindo, Fabio, Siebert, Martin (Eds.), *Developments in Earth and Environmental Sciences. Antarctic Climate Evolution*, vol. 8. Elsevier, The Netherlands, pp. 85–114.
- Chand, S., Minshull, T.A., 2003. Seismic constraints on the effects of gas hydrate on sediment physical properties and fluid flow: a review. *Geofluids* 3, 275–289.
- Chelton, D.B., Schlax, M.C., Witter, D.L., Richman, G.J., 1990. Geosat Altimeter Observations of the Surface Circulation of the Southern Ocean. *Journal of Geophysical Research* 95 (C10), 17877–17903.
- Chough, S.K., Hesse, R., 1985. Contourite from Eirik Ridge, south of Greenland. *Sedimentary Geology* 41, 185–199.
- Cooper, A.K., Barrett, P.J., Hinz, K., Traube, V., Leitchenkov, G., Stagg, H.M.J., 1991. Cenozoic prograding sequences of the Antarctic continental margin: a record of glacio-eustatic and tectonic events. *Marine Geology* 102, 175–213.
- Eagles, G., 2003. Plate tectonics of the Antarctic–Phoenix plate system since 15 Ma. *Earth and Planetary Science Letter* 88, 289–307.
- Eagles, G., Livermore, R.A., Fairhead, J.D., Morris, P., 2005. Tectonic evolution of the west Scotia Sea. *Journal of Geophysical Research* 11, B02401. doi:10.1029/2004JB003154.
- Evans, D., Stoker, M.S., Cramp, A., 1998. Geological processes on continental margins: Sedimentation, mass-wasting and stability: an introduction. In: Stoker, M.S., Evans, D., Cramp, A. (Eds.), *Geological Processes on Continental Margins: Sedimentation, Mass-Wasting and Stability*. Geological Society Special Publication, vol. 129, pp. 1–4.
- Ewing, M., Lonardi, A.G., 1971. Sediment Transport and Distribution in the Argentine Basin. 5. Sedimentary structure of the Argentine Margin, Basin, and related provinces. In: Ahrens, L., Press, F., Runcorn, S., Urey, H. (Eds.), *Physics and Chemistry of the Earth*, 8. Pergamon Press, Oxford, pp. 125–251.
- Faugères, J.C., Stow, D.A.V., 1993. Bottom current controlled sedimentation: a synthesis of the contourite problem. *Sedimentary Geology* 82, 287–297.
- Faugères, J.C., Stow, A.V., 2008. Contourite drifts: nature, evolution and controls. In: Rebesco, M., Camerlenghi, A. (Eds.), *Contourites. Developments in Sedimentology*, vol. 60. Elsevier, pp. 259–288.
- Faugères, J.C., Mezerais, M.L., Stow, D.A.V., 1993. Contourite drift types and their distribution in the North and South Atlantic Ocean basins. *Sedimentary Geology* 82 (1–4), 189–203.
- Faugères, J.C., Stow, D.A.V., Imbert, P., Viana, A., 1999. Seismic features diagnostic of contourite drifts. *Marine Geology* 162, 1–38.
- Figueroa, D., Marshall, P., Prayitno, W., 2005. Cuencas Atlánticas de aguas profundas: principales playas. APA, VI Congress. Abstract volume, 11 pp.
- Flood, R.D., Giosan, L., 2002. Migration history of a fine-grained abyssal sediment wave on the Bahama Outer Ridge. *Marine Geology* 192, 259–273.
- Flood, R.D., Shor, A.N., 1988. Mud waves in the Argentine Basin and their relationship to regional bottom circulation patterns. *Deep-Sea Research* 35 (6), 943–971.
- Franke, D., Neben, S., Ladage, S., Schreckenberger, B., Hinz, K., 2007. Margin segmentation and volcano-tectonic architecture along the volcanic margin of Argentina/Uruguay, South Atlantic. *Marine Geology* 44, 46–67.
- García, M., Hernández-Molina, F.J., Llave, E., Stow, D.A.V., León, R., Fernández-Puga, M.C., Díaz del Río, V., Somoz, L., 2009. Contourite erosive features caused by the Mediterranean Outflow Water in the Gulf of Cadiz: Quaternary tectonic and oceanographic implications. *Marine Geology* 257, 24–40.
- Gardner, G.H.F., Gardner, L.W., Gregory, A.R., 1974. Formation velocity and density – the diagnostic basics for stratigraphic traps. *Geophysics* 39 (6), 770–780.
- Georgi, D.T., 1981b. On the relationship between the large-scale property variations and fine structure in the circumpolar deep water. *Journal of Geophysical Research* 86 (C7), 6556–6566.
- Georgi, D.T., 1981a. Circulation of bottom water in the south-western South Atlantic. *Deep-Sea Research* 28, 959–979.

- Gładczenko, T.P., Hinz, K., Eldholm, O., Meyer, H., Neben, S., Skogseid, J., 1997. South Atlantic volcanic margins. *Journal of the Geological Society of London* 154, 456–470.
- Haq, B.U., Hardenbol, J., Vail, P.R., 1987. Chronology of fluctuating sea levels since the Triassic. *Science* 235, 1156–1167.
- Heezen, B.C., Tharp, M., 1977. World Ocean Floor Panorama. In Full Color, Painted by H. Ber Mercator Projection, Scale 1: 23,230,300, 46"×76". Marie Tharp, South Nyack, New York, 1 sheet.
- Henriet, J.P., Mienert, J. (Eds.), 1998. Gas Hydrates. Relevance to World Margin Stability and Climate Change. Geological Society, London, Special Publication, 137, 338 pp.
- Hernández-Molina, F.J., Llave, E., Stow, D.A.V., 2008a. Continental slope contourites. In: Rebesco, M., Camerlenghi, A. (Eds.), Contourites. Developments in Sedimentology, vol. 60. Elsevier, pp. 379–407.
- Hernández-Molina, F.J., Maldonado, A., Stow, D.A.V., 2008b. Abyssal Plain contourites. In: Rebesco, M., Camerlenghi, A. (Eds.), Contourites. Developments in Sedimentology, vol. 60. Elsevier, pp. 347–377.
- Hernández-Molina, F.J., Llave, E., Stow, D.A.V., García, M., Somoza, L., Vázquez, J.T., Lobo, F., Maestro, A., Díaz del Río, V., León, R., Medialdea, T., Gardner, J., 2006. The contourite depositional system of the Gulf of Cadiz: a sedimentary model related to the bottom current activity of the Mediterranean Outflow Water and the continental margin characteristics. *Deep-Sea Research II* 53, 1420–1463.
- Hernández-Molina, F.J., Paterlini, M., Violante, R., Marshall, P., de Isasi, M., Somoza, L., Rebesco, M., 2009. A contourite depositional system on the Argentine slope: an exceptional record of the influence of Antarctic water masses. *Geology* 137 (6), 507–510.
- Hinz, K., Popovici, A., et al., 1988. Report on Multichannel Seismic Reconnaissance Survey of the Argentine Eastern Continental Margin by S.V. Explora. BGR-report 102.371, 76 p.
- Hinz, K., Roeser, H., Meyer, H., Franke, D., 2000. Research Cruise BGR98 – Geophysical and Geochemical Studies Off Argentina with M/V Akademik Lazarev. BGR-report 0 120.364, 97 pp.
- Hinz, K., Neben, S., Schreckenberger, B., Roeser, H.A., Block, M., Goncalves de Souza, K., Meyer, H., 1999. The Argentine continental margin north of 48°S: sedimentary successions, volcanic activity during break-up. *Marine and Petroleum Geology* 16, 1–25.
- Horozal, S., Lee, G.H., Yi, B.Y., Yoo, D.G., Park, K.P., Lee, H.Y., Kim, L.H., Lee, K.K., 2008. Seismic indicators of gas hydrate and associated gas in the Ulleung Basin, East Sea (Japan Sea) and implications of heat flows derived from depths of the bottom-simulating reflector. *Marine Geology* 258, 126–138.
- Hunter, S., 2008. Spatial and Temporal Variation in m, rite Sedimentation; Link to Variation in Palaeocirculation. PhD thesis, University of Southampton. 187 pp.
- Hunter, S.E., Wilkinson, D., Stanford, J., Stow, D.A.V., Bacon, S., Akhmetzhanov, A.M., Kenyon, N.H., 2007. The Eirik Drift: a long-term barometer of north Atlantic deepwater flux south of Cape Farewell, Greenland. In: Viana, A., Rebesco, M. (Eds.), Economic and Paleooceanographic Importance of Contourites. Geological Society of London Special Publication, vol. 276, pp. 245–263.
- Jansen, E., Raymo, M.E., 1996. Leg 162: New Frontiers on past climates. In: Jansen, E., Raymo, M.E., Blum, P., et al. (Eds.), Proceeding of the Ocean Drilling Program, Initial Reports, vol. 162, pp. 5–20.
- Joseph, L.H., Rea, D.K., van der Pluijm, B.A., 2004. Neogene history of the Deep Western Boundary Current at Rekohu sediment drift, Southwest Pacific (ODP Site 1124). *Marine Geology* 205, 185–206.
- Kennett, J.P., 1982. *Marine Geology*. Prentice Hall, 813 pp.
- Klaus, A., Ledbetter, M.T., 1988. Deep-sea sedimentary processes in the Argentine Basin revealed by high-resolution seismic records (3.5 kHz echograms). *Deep-Sea Research* 40, 899–917.
- Knutz, P.C., 2008. Paleooceanographic significance of Contourite Drifts. In: Rebesco, M., Camerlenghi, A. (Eds.), Contourites. Developments in Sedimentology, vol. 60. Elsevier, pp. 511–535.
- Laberg, J.S., Stoker, M.S., Torbjørn Dahlgren, K.L., de Haas, H., Hafliðason, H., Hjelstuen, B.O., Nielsen, T., Shannon, P.M., Vorren, T.O., van Weering, T.C.E., Ceramicola, S., 2005. Cenozoic along slope processes and sedimentation on the NW European Atlantic margin. *Marine Petroleum Geology* 22 (1), 069–1088.
- Lagabriele, Y., Goddéri, Y., Donnadieu, Y., Malavieille, J., Suarez, M., 2009. The tectonic history of Drake Passage and its possible impacts on global climate. *Earth and Planetary Science Letters* 279, 197–211.
- Latimer, J.C., Fillipelli, G.M., 2002. Eocene to Miocene terrigenous inputs and export production: geochemical evidence from ODP Leg 177, Site 1090. *Paleoceanography, Palaeoclimatology, Palaeoecology* 182, 151–164.
- Lawver, L.A., Gahagan, L.M., 2003. Evolution of Cenozoic seaways in the circum-Antarctic region. *Paleoceanography, Palaeoclimatology, Palaeoecology* 198, 11–37.
- Le Pichon, X., Eitrem, S.L., Ludwig, W.L., 1971. Sediment transport & distribution in the Argentine basin. 1. Antarctic bottom current passage through the Falkland fracture zone. In: Ahrens, L.H., Press, F., Runcorn, S.K., Urey, H.C. (Eds.), *Physics and Chemistry of the Earth*, 8. Pergamon Press, pp. 2–28.
- Ledbetter, M.T., Ciesielski, P.F., 1986. Post-miocene disconformities and paleoceanography in the Atlantic sector of the Southern Ocean. *Paleoceanography, Palaeoclimatology, Palaeoecology* 52 (3–4), 185–214.
- Light, M.P.R., Keeley, M.L., Maslanjy, M.P., Urien, C.M., 1993. The tectono-stratigraphic development of Patagonia, and its relevance to hydrocarbon exploration. *Journal of Petroleum Geology* 16 (4), 465–482.
- Lima, A.F., 2003. Comparação dos sistemas sedimentares profundos da Bacia Sudeste-Sul do Brasil com ênfase no sistema misto Colúmbia. PhD thesis, Universidade de São Paulo, Brazil, 252 pp.
- Livermore, R., Balanyá, J.C., Maldonado, A., Martínez, J.M., Rodríguez-Fernández, J.R., Sánz de Galdeano, C., Galindo Zaldívar, J., Jabaloy, A., Barnolas, A., Somoza, L., Hernández-Molina, F.J., Suriñach, E., Viseras, C., 2000. Autopsy of a dead spreading center: the Phoenix Ridge, Drake Passage, Antarctica. *Geology* 28 (7), 607–610.
- Livermore, R., Eagles, G., Morris, P., Maldonado, A., 2004. Shackleton Fracture Zone: no barrier to early circumpolar ocean circulation. *Geology* 32, 797–800.
- Livermore, R., McAdoo, D., Marks, K., 1994. Scotia Sea tectonics from high-resolution satellite gravity. *Earth and Planetary Science Letter* 123, 255–268.
- Llave, E., Hernández-Molina, F.J., Somoza, L., Díaz-del-Río, V., Stow, D.A.V., Maestro, A., Alveirinho Dias, J.M., 2001. Seismic stacking pattern of the Faro-Albufeira contourite system (Gulf of Cadiz): a Quaternary record of paleoceanographic and tectonic influences. *Marine Geophysical Researches* 22, 487–508.
- Llave, E., Hernández-Molina, F.J., Somoza, L., Stow, D., Díaz del Río, V., 2007. Quaternary evolution of the contourite depositional system in the Gulf of Cadiz. In: Viana, A., Rebesco, M. (Eds.), Economic and Paleooceanographic Importance of Contourites. Geological Society of London, Special Publication, vol. 276, pp. 49–79.
- Lonardi, A.G., Ewing, M., 1971. Sediment Transport and Distribution in the Argentine Basin. 4. Bathymetry of the Continental margin Argentine Basin and Other related provinces. Canyons and Sources of Sediments. In: Ahrens, L., Press, F., Runcorn, S., Urey, H. (Eds.), *Physics and Chemistry of the Earth*, 8. Pergamon Press, Oxford, pp. 81–121.
- Loseth, H., Gading, M., Wensaas, L., 2009. Hydrocarbon leakage interpreted on seismic data. *Marine and Petroleum Geology* 26, 1304–1319.
- Lyatsky, H., Pana, D., Olson, R., Godwin, L., December 2004. Detection of subtle basement faults with gravity and magnetic data in the Alberta Basin, Canada: a data-use tutorial. *The Leading Edge*, 1282–1288.
- Maldonado, A., Barnolas, A., Bohoyo, F., Escutia, C., Galindo-Zaldívar, J., Hernández-Molina, F.J., Jabaloy, A., Lobo, F., Nelson, C.H., Rodríguez-Fernández, J., Somoza, L., Vázquez, J.T., 2005. Miocene to recent contourite drifts development in the northern Weddell Sea (Antarctica). In: Florindo, F., Harwood, D.M., Wilson, G.S. (Eds.), Long-term Changes in Southern High-latitude Ice Sheets and Climate: The Cenozoic History. *Global and Planetary Change* 45, 99–129.
- Maldonado, A., Barnolas, A., Bohoyo, F., Galindo-Zaldívar, J., Hernández-Molina, F.J., Lobo, F., Rodríguez-Fernández, J., Somoza, L., Vázquez, J.T., 2003. Contourite deposits in the central Scotia Sea: the importance of the Antarctic Circumpolar Currents and the Weddell Gyre flows. *Paleoceanography, Palaeoclimatology and Palaeoecology* 198, 187–221.
- Maldonado, A., Bohoyo, F., Galindo-Zaldívar, J., Hernández-Molina, F.J., Jabaloy, A., Lobo, F., Rodríguez-Fernández, J., Suriñach, E., Vázquez, J.T., 2006. Ocean basins near the Scotia and Antarctic plate boundary: influence of the tectonics and paleoceanography on the Cenozoic evolution. *Marine Geophysical Research* 27, 83–107.
- Malumian, N., Olivero, E.B., 2005. El Oligoceno–Plioceno marino del Rio Irigoyen, costa atlántica de Tierra del Fuego, Argentina: una conexión atlántico–pácifica. *Revista Geologica de Chile* 32 (1), 117–129.
- Manley, P.L., Flood, R.D., 1989. Anomalous sound velocity in near-surface, organic-rich gassy sediments in the central Argentine Basin. *Deep-Sea Research* 36, 611–623.
- Manley, P.L., Flood, R.D., 1993. Project MUDWAVES. *Deep-Sea Research II* 40 (4/5), 851–857.
- Masson, D.G., 2001. Sedimentary processes shaping the eastern slope of the Faeroe–Shetland Channel. *Continental Shelf Research* 21, 825–857.
- McCave, I.N., Tucholke, B.E., 1986. Deep current controlled sedimentation in the western North Atlantic. In: Vogt, P.R., Tucholke, B.E. (Eds.), *The Western North Atlantic Region. The Geology of North America*, vol. M. Geological Society of America, Boulder (CO), pp. 451–468.
- Mézerai, M.L., 1991. Accumulations sédimentaires profondes turbiditique deepsea fan du Cap Ferret et contouritique bassin sudbresilien: géométrie, facies, édification. These, Univ. Bordeaux I, 606, 301 pp.
- Mézerai, M.L., Faugères, J.C., Figueiredo y, A., Masse, L., 1993. Contour current accumulation off Vema Channel mouth, southern Brazil Basin. *Sedimentary Geology* 82 (1–4), 173–188.
- Mouzo, F.H., 1982. *Geología Marítima y fluvial*. In: *Historia Marítima Argentina*, Tomo I, Buenos Aires 47–117 pp.
- Neben, S., Schreckenberger, B., 2005. Geophysical investigations offshore Argentine and Uruguay ARGURU. Cruise Report BGR Cruise BGR04, 99 pp.
- Nelson, C.H., Baraza, J., Maldonado, A., 1993. Mediterranean undercurrent sandy contourites, Gulf of Cadiz, Spain. *Sedimentary Geology* 82, 103–131.
- Nelson, C.H., Baraza, J., Maldonado, A., Rodero, J., Escutia, C., Barber, J.H., 1999. Influence of the Atlantic inflow and Mediterranean outflow currents on Late Quaternary sedimentary facies of the Gulf of Cadiz continental margin. *Marine Geology* 155, 99–129.
- Niemi, T.M., Ben-Avraham, Z., Hartnady, C.J.H., Reznikov, M., 2000. Post-Eocene seismic stratigraphy of the deep ocean basin adjacent to the southeast African continental margin: a record of geostrophic bottom current systems. *Marine Geology* 162, 237–258.
- Nisancioglu, K.H., Raymo, M.E., Stone, P.H., 2003. Reorganization of Miocene deep water circulation in response to the shoaling of the Central American Seaway. *Paleoceanography* 18 (1), 1006. doi:10.1029/2002PA000767.
- Onken, R., 1995. The spreading of lower circumpolar deep water in the Atlantic Ocean. *Journal of Physical Oceanography* 25 (12), 3051–3063.



- Parker, R.L., 1973. The rapid calculation of potential anomalies. *Geophysical Journal of the Royal Astronomical Society* 31, 447–455.
- Parker, G., Paterlini, M.C., Violante, A., 1997. El fondo marino. In: *El Mar argentino y sus Recursos Marinos Pesqueros*, 1. INIDEP, Mar del Plata, 65–87 pp.
- Parker, G., Violante, A., Paterlini, M.C., 1996. Fisiografía de la Plataforma Continental. In: Ramos, V.A., Turic, M.A. (Eds.), *Geología y Recursos Naturales de la Plataforma Continental Argentina*, XIII Congreso Geológico Argentino y III Congreso de Exploración de Hidrocarburos, Buenos Aires, 1996, vol. 1. Asociación Geológica Argentina-Instituto Argentino del Petróleo, Relatorio, pp. 1–16.
- Pawlowski, R., June 2008. The use of gravity anomaly data for offshore continental margin demarcation. *The Leading Edge*, 722–727.
- Pecher, I.A., Holbrook, W.S., 2000. Seismic methods for detecting and quantifying marine methane hydrate/free gas reservoirs. In: Max, M.D. (Ed.), *Natural Gas Hydrate in Oceanic and Permafrost Environments*. Kluwer Academic Publishers, Netherlands, pp. 275–294.
- Pfuhl, H.A., McCave, I.N., 2005. Evidence for late Oligocene establishment of the Antarctic Circumpolar Current. *Earth and Planetary Science Letter* 235, 715–728.
- Piola, A.R., Matano, R.P., 2001. Brazil and Falklands (Malvinas) currents. In: Steele, J. H., Thorpe, S.A., Turekian, K.K. (Eds.), *Encyclopedia of Ocean Sciences*, vol. 1. Academic Press, London, pp. 340–349.
- Piola, A.R., Rivas, A., 1997. Corrientes en la plataforma continental. In: Boschi, E.E. (Ed.), *Antecedentes históricos de las exploraciones en el mar y las características ambientales*. El Mar Argentino y sus recursos pesqueros, Tomo 1. Instituto Nacional de Investigación y Desarrollo Pesquero, Secretaría de Agricultura, Ganadería, Pesca y Alimentación, Mar del Plata, República Argentina, pp. 119–132.
- Ramos, V.A., 1996. Evolución tectónica de la Plataforma Continental. XIII° Congreso Geológico Argentino – III° Congreso de Exploración de Hidrocarburos. In: Ramos, V., Turic, M.A. (Eds.), *Geología y Recursos de la Plataforma Continental*. Asociación Geológica Argentina-Instituto Argentino del Petróleo, Relatorio, pp. 85–404.
- Rebesco, M., 2005. Contourites. In: Selley, R.C., Cocks, L.R.M., Plimer, I.R. (Eds.), *Encyclopedia of Geology*, vol. 4. Elsevier, London, pp. 513–527.
- Rebesco, M., Camerlenghi, A. (Eds.), 2008. Contourites. *Developments in Sedimentology*, vol. 60. Elsevier, p. 688 pp.
- Rebesco, M., Pudsey, C., Canals, M., Camerlenghi, A., Barker, P., Estrada, F., Giorgetti, A., 2002. Sediment Drift and Deep-Sea Channel Systems, Antarctic Peninsula Pacific Margin. In: Stow, D.A.V., Pudsey, C.J., Howe, J.A., Faugères, J.C., Viana, A.R. (Eds.), *Deep-Water Contourite Systems: Modern Drifts and Ancient Series, Seismic and Sedimentary Characteristics*. Geological Society of London, *Memoirs* 22, 353–371.
- Rebesco, M., Stow, D., 2001. Seismic expression of contourites and related deposits: a preface. *Marine Geophysical Researches* 22, 303–308.
- Reid, J.L., 1989. On the total geostrophic circulation of the South Atlantic Ocean: flow patterns, tracers, and transports. *Progress in Oceanography* 23, 149–244.
- Reid, J.L., 1996. On the circulation of the South Atlantic. In: Wefer, G., Berger, W., Siedler, G., Webb, J. (Eds.), *The South Atlantic – Present and Past Circulation*. Springer Verlag, Berlin, pp. 13–44.
- Saunders, P.M., King, B.A., 1995. Bottom current derived from a Shipborne ADCP on WOCE Cruise A11 in the South Atlantic. *Journal of Physical Oceanography* 25, 329–347.
- Schlüter, P., Uenzelmann-Neben, G., 2007. Seismostratigraphic analysis of the Transkei Basin: a history of deep sea controlled sedimentation. *Marine Geology* 240, 99–111.
- Schlüter, P., Uenzelmann-Neben, G., 2008. Indications for bottom current activity since Eocene times: The climate and ocean gateway archive of the Transkei Basin, South Africa. *Global and Planetary Change* 60 (3–4), 416–428.
- Schümann, T., 2002. The Hydrocarbon Potential of the Deep Offshore along the Argentine Volcanic Margin – A Numerical Simulation. Ph.D. thesis, Rheinisch-Westfälischen Technischen Hochschule Aachen.
- Schümann, T., Ellouz, N., Franke, D., Hinz, K., Littke, R., 2002. The Hydrocarbon Potential of the Deep offshore along the Argentine Passive Volcanic Margin – A Basin Modeling Study. AAPG Hedberg Conference, Hydrocarbon Habitat of Volcanic Rifted Passive Margins, September, 8–11, 2002. Stavanger, Norway.
- Speer, K., Zenk, W., Siedler, G., Pätzold, J., Heidland, K., 1992. First resolution of flow through the Hunter Channel in the South Atlantic. *Earth and Planetary Science Letter* 113, 287–292.
- Stoker, M.A., Praeg, D., Hjelstuen, B.O., Laberg, J.S., Nielsen, T., Shannon, P.M., 2005. Neogene stratigraphy and the sedimentary and oceanographic development of the NW European Atlantic margin. *Marine and Petroleum Geology* 22, 977–981.
- Stow, D.A.V., 1994. Deep sea processes of sediment transport and deposition. In: Kenneth, P. (Ed.), *Sediment Transport and Depositional Processes*. Blackwell Scientific Publications, Oxford, pp. 257–291.
- Stow, D.A.V., Faugères, J.C., Howe, J.A., Pudsey, C.J., Viana, A., 2002a. Contourites, bottom currents and deep-sea sediment drifts: current state-of-the-art. In: Stow, D.A.V., Pudsey, C.J., Howe, J.A., Faugères, J.C., Viana, A.R. (Eds.), *Deep-Water Contourite Systems: Modern Drifts and Ancient Series, Seismic and Sedimentary Characteristics*. Geological Society of London, *Memoirs* 22, 7–20.
- Stow, D.A.V., Hunter, S., Wilkinson, D., Hernández-Molina, F.J., 2008. The nature of contourite deposition. In: Rebesco, M., Camerlenghi, A. (Eds.), *Contourites. Developments in Sedimentology*, vol. 60. Elsevier, pp. 143–156.
- Stow, D.A.V., Mayall, M. (Eds.), 2000. *Deep-water Sedimentary Systems*. *Marine and Petroleum Geology* 17, 342 pp.
- Stow, D.A.V., Pudsey, C.J., Howe, J.A., Faugères, J.C., Viana, A.R. (Eds.), 2002b. Deep-water contourite systems: modern drifts and ancient series, seismic and sedimentary characteristics. *Geological Society of London, Memoirs*, 22, p. 464.
- Stow, D.A.V., Hernández-Molina, F.J., Llave, E., Sayago, M., Díaz del Río, V., Branson, A., 2009. Bedform-velocity matrix: the estimation of bottom current velocity from bedform observations. *Geology* 37 (4), 327–330.
- Supko, P.R., Perch-Nielsen, K., 1977. General Synthesis of Central and South Atlantic Drilling Results/Deep Sea Drilling Project [Initial Report of the Deep Sea Drilling Project], vol. 39. U.S. Government Printing Office, Washington, 1099–1132 pp.
- Sykes, T.J.S., Ramsay, T.S., Kidd, R.B., 1998. Southern hemisphere Miocene bottom-water circulation: a palaeobathymetric analysis. In: Cramp, A., MacLeod, C.J., Lee, S.V., Jones, E.J.W. (Eds.), *Geological Evolution of Ocean Basin: Results from the Ocean Drilling Program*, vol. 131. Geological Society of London, pp. 43–54.
- Talwani, M., Ewing, M., 1960. Rapid computation of gravitational attraction of three-dimensional bodies of arbitrary shape. *Geophysics* 25 (1), 203–225.
- Uenzelmann-Neben, G., 2001. Seismic characteristics of sediment drifts: an example from the Agulhas Plateau, southwest Indian Ocean. *Marine Geophysical Research* 22, 323–343.
- Uenzelmann-Neben, G., 2002. Contourites on the Agulhas Plateau, SW Indian Ocean: indications for the evolution of current since Palaeogene times. In: Stow, D.A.V., Pudsey, C.J., Howe, J.A., Faugères, J.C., Viana, A.R. (Eds.), *Deep-Water Contourite Systems: Modern Drifts and Ancient Series, Seismic and Sedimentary Characteristics*. Geological Society of London, *Memoirs* 22, 271–288.
- Urien, C.M., 2001. Present and future petroleum provinces of Southern South America. In: Downey, M.W., Threet, J.C., Morgan, W.A. (Eds.), *Petroleum Provinces of the Twenty-first Century*. American Association of Petroleum Geologists, *Memoir* 74, 373–402.
- Urien, C.M., Zambrano, J.J., 1996. Estructura de la Plataforma Continental. In: Ramos, V., Turic, M.A. (Eds.), *Geología y Recursos de la Plataforma Continental*. Asociación Geológica Argentina-Instituto Argentino del Petróleo, Relatorio, pp. 29–66. XIII° Congreso Geológico Argentino - III° Congreso de Exploración de Hidrocarburos.
- Urien, C.M., Martins, L.R., Zambrano, J.J., 1976. The geology and tectonic framework of Southern Brazil, Uruguay and North Argentina continental margin: their behavior during the Southern Atlantic opening Continental Margins of the Atlantic Type. *Anais da Academia Brasileira de Ciências* 48, 365–376. Sao Paulo.
- Van Andel, T.J.H., Thiede, J., Sclater, J.G., Hay, W.W., 1977. Depositional history of the South Atlantic during the last 125 Million Years. *Journal of Geology* 85, 651–698.
- Vanneste, M., Jeffrey, P., De Batist, M., Klerkx, J., 2002. A typical heat flow near gas hydrate irregularities and cold seeps in the Baikal Rift Zone. *Marine and Petroleum Geology* 19, 1257–1274.
- Viana, A.R., 2008. Economic relevance of contourites. In: Rebesco, M., Camerlenghi, A. (Eds.), *Contourites*. Elsevier, *Developments in Sedimentology*, Vol. 60, Elsevier, pp. 493–510.
- Viana, A.R., Figueiredo, A.G., Faugères, J.C., Lima, A.F., Gonthier, E., Brehme, I., Zaragosi, S., 2003. The São Paulo Tomé deep-sea turbidite system (South Brazilian basin): cenozoic seismic stratigraphy and sedimentary processes. *American Association of Petroleum Geologists Bulletin* 87, 873–894.
- Viana, A.R., Almeida Jr., W., Nunes, C.V., Bulhões, E.M., 2007. The economic importance of contourites. In: Viana, A., Rebesco, M. (Eds.), *Economic and Paleooceanographic Significance of Contourites*. Geological Society of London Special Publication, vol. 276, pp. 1–23.
- Von Lom-Keil, H., Spieß, V., Hopfauf, V., 2002. Fine-grained sediment waves on the western flank of the Zapiola Drift, Argentine Basin: evidence for variations in Late Quaternary bottom flow activity. *Marine Geology* 192, 239–258.